Transportation Research Part C 141 (2022) 103734

Contents lists available at ScienceDirect

Transportation Research Part C

journal homepage: www.elsevier.com/locate/trc

Resilient airline scheduling to minimize delay risks

Deniz Şimşek [a], M. Selim Aktürk [b,*]

[a] Kellogg School of Management, Northwestern University, Evanston, IL, 60201, USA
[b] Department of Industrial Engineering, Bilkent University, Ankara 06800, Turkey

ARTICLE INFO

Keywords:
Resilient airline scheduling
Aircraft routing and fleeting
Cruise time controllability
Chance constraints
Second order cone programming

ABSTRACT

Airlines tend to design their flights schedules with the primary concern of the minimization of operational costs. However, the recently emerging idea of resilient scheduling defined as staying operational in case of unexpected disruptions and adaptability should be of great importance for airlines as well due to the high opportunity costs caused by the flight cancellations and passenger inconvenience caused by delays in the schedule. In this study, we integrate resilient airline schedule design, aircraft routing and fleet assignment problems with uncertain non-cruise times and controllable cruise times. We follow a data-driven method to estimate flight delay probabilities to calculate the airport congestion coefficients required for the probability distributions of non-cruise time random variables. We formulate the problem as a bi-criteria nonlinear mixed integer mathematical model with chance constraints. The nonlinearity caused by the fuel consumption and CO_2 emission function associated with the controllable cruise times in our first objective is handled by second order conic inequalities. We minimize the total absolute deviation of the aircraft path variability's from the average in our second objective to generate balanced schedules in terms of resilience. We compare the recovery performances of our proposed schedules to the minimum cost schedules by a scenario-based posterior analysis.

1. Introduction

Airlines are one of the most complex industries which consist of large scale networks. Therefore, they need to schedule their limited resources effectively. Besides the complexity of the airline scheduling problems, airlines run in an uncertain environment which causes the airlines to be open to unpredicted changes. So, airlines should also be able to manage disruptions. This situation forces airlines to create schedules which are capable of adapting or withstanding disruptions.

Different types of schedules are defined in the literature regarding airline scheduling. The most common term that we can use for an airline schedule is "robust". Cook et al. (2016) define robustness as the resistance to withstand stresses beyond normal limits. There are several studies available in the literature which aim to create robust airline schedules and aim to increase the robustness through increasing the passenger connection service levels. As new optimization and prediction techniques are developed, other terms started to be used in this sector as well. Lufthansa (2018) mentions in their blog that minimizing the delay risks can be achieved through the use of resilient scheduling rather than robust scheduling. Resilience can be defined as the ability of a system to withstand and stay operational in the face of an unexpected disturbance or unpredicted change as discussed in Wang et al. (2019).

In fact, resilience is a more comprehensive term than robustness and where they differ is that robust schedule design aims to accommodate any uncertain future events such that the initially desired future state can still be achieved whereas resilient schedule design aims to adapt to disruptions by changing its methods while continuing to operate and to be able to return to the original state

* Corresponding author.
E-mail address: akturk@bilkent.edu.tr (M.S. Aktürk).

https://doi.org/10.1016/j.trc.2022.103734
Received 22 September 2021; Received in revised form 27 April 2022; Accepted 15 May 2022

of the system or move to a new desirable state after disruptions. Clearly, resilient schedule design is an emerging area and not much of a literature has been developed where resilience is considered as an objective besides the total cost or profit of the generated schedules. This study aims to create resilient airline schedules by considering the trade-off between decreasing the variability of the system and minimizing the operational cost of the generated schedules.

In our study, we propose an integrated approach to resilient airline scheduling problem to minimize delay risks. In contrary to the single-criterion approaches which focus on minimizing the total costs of schedules, we follow a bi-criteria framework to increase the resilience of the system while keeping the operational cost within acceptable limits. To achieve that, we introduce the variability of the system as an indicator of resilience. We propose that the variability of the system depends on the several factors, such as the airport congestion, the fleet assignments due to the different characteristics of the aircraft, and also the flight departure times which affect the uncertain non-cruise times. Thus, we calculate the variability of an aircraft path based on its characteristics and flight assignments. Then, our proposed objective is to minimize total absolute deviation of the variability's of aircraft paths from their average such that the resulting schedule would be as balanced as possible. The motivation behind aiming for balanced schedules is that the disruptions that we are aiming to handle are uncertain and which aircraft is going to be affected by them cannot be known for sure beforehand. This is the key contribution of this study to the resilient airline scheduling literature.

Another important contribution to the related literature is to incorporate empirical techniques to capture the effects of airport congestion in the random variables that we use for uncertain non-cruise times. We followed a data-driven methodology to estimate departure and arrival delay probabilities of flights which were generally taken as the equal to each other in the existing literature. We also contribute to the literature by introducing a data-driven procedure to calculate turnaround times required to prepare aircraft between consecutive flights which provides a more thoroughgoing way than normalizing the number of passengers visiting the airports as it was done in the literature.

We first propose a bi-objective nonlinear mixed-integer mathematical model with chance constraints. Afterwards, we reformulate it to handle the nonlinearity by using second order conic inequalities, and to handle probabilistic chance constraints by using value-at-risk risk measure to be able to solve the problem via commercial solvers. We also devise a math-heuristic algorithm for larger flight networks, and develop an integrated flight and passenger recovery algorithm in order to evaluate the performance of our proposed formulation via a posterior analysis. Finally, we conducted several what if analyses to gain some managerial insight on the behaviour and performance of our proposed methodology. To summarize, main contributions of this study are as follows:

- In our bi-objective framework, we minimize the variability of the system depending on aircraft characteristics, fleet assignment and schedule design decisions while keeping the operational cost within acceptable limits.
- We propose a novel data-driven methodology for calculating the parameters required for the probability distributions of non-cruise time random variables in which delay probabilities occurred in origin and destination airports are distinguished from each other.
- We utilize value-at-risk risk measure to reformulate the chance constraints.

The remainder of this paper is organized in the following way. In Section 2, we provide a literature review on robust airline scheduling and airline recovery problems. In Section 3, we introduce the proposed bi-criteria nonlinear mixed-integer mathematical model with chance constraints. Section 4 describes the proposed discretized approximation and aircraft swapping algorithm. An extensive computational study is provided in Section 5, along with the empirical study that we conducted on the historical airline on-time performance data. In Section 6, we present the managerial insights gained by the several what if analyses on different problem parameters.

2. Literature review

Although the term "resilience" has been used in network design problems, this is a relatively new idea in airline scheduling. Therefore, we mainly focus on the robust scheduling literature as well as the pioneering works for resilient airline scheduling. In a flight schedule, block times of flights consist of cruise times which can be controlled by adjusting the speed of the aircraft and non-cruise times that are uncertain. Majority of the non-cruise times are allocated to taxi-in and taxi-out times of the aircraft which are subject to high uncertainty so they cause significant delays resulting in passengers missing their flight connections. Because of this uncertainty, many works in the literature focus on robust airline scheduling in order to satisfy passenger connection service levels.

AhmadBeygi et al. (2010) aim to minimize the expected value of delay propagation by modifying the flight departure times to re-allocate the existing slack in the flight networks. Sohoni et al. (2011) develop a comprehensive model that includes block-time uncertainty where they explicitly model block-time distributions through chance constraints while incorporating network service levels. Deshpande and Arıkan (2012) propose a newsvendor framework by constructing overage and shortage costs and also show that the stochastic non-cruise times fit a symmetric Log-Laplace distribution. Duran et al. (2015) propose a mathematical model which inserts slacks into the schedule and speed up the aircraft if necessary as well as using chance constraints on passenger connection service levels. Gürkan et al. (2016) use chance constraints on the passenger connection service levels to generate robust flight sequences together with the aircraft fleeting and routing decisions. Cadarso and De Celis (2017) propose an integrated approach for airline planning where the aim is to update flight schedules when a disruption occurs in a way that the robustness is achieved against demand uncertainty by decreasing the number of mis-connected passengers. Ben Ahmed et al. (2017) propose a hybrid approach to obtain robust decisions for aircraft routing and re-timing through the use of optimization and simulation in terms of the flight delays and their propagation through the flight network.

Recently, there have been few studies which follow data-driven frameworks focusing on flight delay. Arora and Mathur (2020) analyze the impact of delayed departure of flights on their arrivals by multinomial logistic regression. Lambelho et al. (2020) propose a machine-learning based mechanism to assess the flight schedules of airlines with respect to their cancellation and delay predictions. Wang et al. (2021) focus on the importance of the prediction of taxi times, which is important for creating robust schedules due to being a significant portion of the uncertain non-cruise times. Prakash (2020) focuses on generating reliable routes on networks where reliability is defined as the probability of on-time arrival at the destination, given a threshold arrival-time. Xu et al. (2021) propose an integrated robust scheduling approach that decides on the schedule design, fleet assignment, and aircraft routing, while considering the effects of propagated delays.

Some pioneering works which consider the resilience of the airline networks are as follows: Janić (2015) develops a methodology to estimate the resilience of the air transport networks and defines resilience as the ability of the network to neutralize the effects of disruptive events. Clark et al. (2018) consider the resilience of the airport network of the U.S. National Airspace System and propose an approach to characterize the resilience of the airport systems after disruptive events. More recently, Wong et al. (2020) propose a data-driven approach which utilizes the Mahalanobis distance metric to quantify abnormalities across the flight networks.

Since the aim in this study is to create flight schedules such that the schedule responds to unexpected events well with respect to certain performance metrics, airline recovery plays an important role on observing the performance of the schedules under disruptions through posteriori analyses. There is a rich amount of literature on airline disruption management. For an extensive review, the recent work by Hassan et al. (2020) can be referred. Petersen et al. (2021) suggest an optimization approach to integrated airline recovery by decomposing the problem into subproblems such as the schedule recovery problem, the aircraft recovery problem, the crew recovery problem, and the passenger recovery problem. It is important to note that there is a critical trade-off between the fuel consumption (and its adverse impact on surface air quality) and delay minimization. Although flight time controllability is a very popular local recovery strategy in practice to deal with the disruptions, its benefit has been limited because it does not consider networkwide integrated effects. Aktürk et al. (2014) was the first study in which the cruise speed was included as a decision variable in an airline recovery optimization model along with the environmental constraints and cost coefficients. Although optimization techniques are used quite extensively in the airline industry, this was the first implementation of a conic quadratic optimization approach to solve a critical aircraft recovery problem in an optimal manner. Afterwards, Arıkan et al. (2017) extended this study and proposed a new flight network based representation to capture interdependencies between aircraft, crew members and passengers. Recently, Evler et al. (2021) propose a resource-constrained project scheduling problem (RCPSP) to obtain recovery actions for disruptions created due to the unavailability of different resources. They define the resilience as the schedule recovery performance and by providing resilient solutions, they claim that the total cost and delay caused by the schedule deviations are minimized. This study is also one of the recent works that include resilience into the airline planning and scheduling problems which in fact is in line with the scope of our study.

3. Proposed formulation

We consider aircraft routing, fleet assignment and schedule design through flight departure times in an integrated manner while we also handle uncertainty caused by non-cruise times. Given the set of flights to be operated and the set of available aircraft, the problem is to determine the routes of the aircraft, block times of the flights, idle times of the aircraft, and fleet assignments to the determined routes while minimizing the total operational cost as well as the variability of the system. A typical flight involves several stages: taxi-out, takeoff, climb, cruise, descent, final approach, landing, and taxi-in. Although the cruise stage is the most fuel efficient portion of the flight, most of the fuel is burned during this longest stage for a typical flight. There is also little room for planned compression in other stages because they are generally dictated by local traffic and safety considerations. Airlines could adjust the cruise speed by considering a critical trade-off between the fuel consumption (and its adverse impact on surface air quality) and delay minimization during the flight planning stage. In order to take full advantage of cruise time controllability, we need to consider its system-wide integrated effects. The major difficulty with including cruise speed control into our model is that the fuel burn and carbon emissions are nonlinear in cruise speed. Therefore, we have taken cruise time as a decision variable (along with the inserted idle times, if any) that directly affects the block times and departure times as well. On the other hand, other stages of the block time, denoted as the non-cruise times, are assumed to be random variables in our study. In sum, the block time of each flight consists of cruise and non-cruise times. Cruise times are controllable in albeit of fuel consumption and CO_2 emission costs, whereas non-cruise times are random variables which are the main source of uncertainty in the system.

The variability of the system depends mainly on the congestion levels of origin and destination airports which affect the non-cruise times of flights. Since the congestion levels at the airports are significantly affected by the time of the day, scheduled departure and arrival times of the flights play an important role on the variability of the system. Minimization of the variability level through the decision of scheduled times requires adjusting the cruise times and idle times of the flights both of which are controllable in our study. Besides the scheduled times, we also consider the aircraft assignments to the flights while calculating the variability of the whole system. Then, we aim to distribute the variability contained in the system in a balanced way such that each aircraft path has a variability value as close to each other as possible. In order to achieve that, in the second objective of our mathematical model, we minimize the absolute deviation of the aircraft path variability's from the average.

We claim that minimizing the variability of system and distributing it as equally as possible throughout all the available aircraft paths increase the resilience of the schedule. We can define increasing the resilience in this context as decreasing the vulnerability of the schedule to unexpected changes in the non-cruise times. Then, to justify the previous claim, the entire schedule can be considered as a queueing system with multiple queues where each aircraft represents a server and each flight assigned to the

aircraft is a job in the queue of that aircraft. When we fix the scheduled arrival times of flights, time between the departure of two consecutive flights is analogous to a deterministic interarrival time. Furthermore, the sum of cruise and non-cruise times is analogous to a random service time because of the uncertainty in non-cruise time. Then, we notice that adjusting the departures of flights intelligently enables us to utilize the aircraft more effectively. For instance, inserting idle times increases the interarrival times, which is equivalent to decreasing the arrival rate for the queue. This clearly decreases the utilization of the server. We know from the fundamental queueing results that if the server is utilized fully, then the expected waiting time of the jobs grows to infinity in the long run. In our context, waiting time is analogous to a departure delay. By optimizing the utilization levels of the aircraft, we avoid having propagated delays in the long run since we can achieve finite expected waiting times. Although we consider a daily planning horizon, this work can be extended to capture longer horizons which is more in line with the long run expected waiting time results of queueing theory. Therefore, it decreases the vulnerability of the entire schedule which means that the resilience of the system can be improved through this method. In addition, distributing the variability among the aircraft paths in a balanced way prevents us from having some aircraft idle for long duration while some other having long propagated delays due to high utilization rates. This in fact makes the schedule less vulnerable to unexpected disruptions since it is not known beforehand that which aircraft or airport is going to be disrupted.

Together with this motivation, we constructed a methodology to capture the aforementioned key points. In the remainder of this section; we first introduce the proposed mathematical model, and then the random variable denoting the non-cruise times with its mathematical properties.

Sets:

T : set of aircraft
F : set of all flight legs
B : set of airports
A : set of all possible consecutive flight pairs
US^i : set of flights which can connect to flight i, $i \in F$
DS^i : set of flights which can flight i can connect to, $i \in F$
$F_e^t,\ F_s^t$: set of flights which aircraft t can use as the first and last flight in the schedule, $t \in T$

Parameters:

$Idle_t$: cost of idle time of aircraft $t \in T$ per minute
c_{fuel} : cost of fuel per ton of fuel consumption
c_{CO_2} : cost of emission per ton of aircraft CO_2 emission
Dem_i : passenger demand of flight $i \in F$
Cap_t : seat capacity of aircraft $t \in T$
$Cspl_i$: opportunity cost of a spilled passenger of flight $i \in F$
$O_i,\ D_i$: origin and destination airports of flight $i \in F$
NC_i : random parameter denoting the non-cruise time of flight $i \in F$
TA_{ij} : turnaround time needed to prepare aircraft between flights $(i, j) \in A$
λ_t : total available cruise time of aircraft t on a day, $t \in T$
bf_t : base value for aircraft $t \in T$
e_b : airport congestion coefficient of airport $b \in B$
$f_i^l,\ f_i^u$: lower and upper time limits on the cruise time of flight $i \in F$
$d_i^l,\ d_i^u$: lower and upper time limits on the departure time of flight $i \in F$
γ_i : desired probability level for the chance constraint for flight $i \in F$

Decision Variables:

d_i : departure time of flight $i \in F$
s_i^t : idle time of aircraft t after flight i, $t \in T,\ i \in F$
f_i^t : cruise time of flight i performed by aircraft t, $i \in F,\ t \in T$
q_i : scheduled block time of flight $i \in F$
x_{ij}^t : 1 if flight i is followed by flight j performed by aircraft t, $i \in F,\ j \in F,\ t \in T,$ and 0 o.w.
y_i^t : 1 if flight i is the first flight performed by aircraft t, $i \in F,\ t \in T,$ and 0 o.w.
z_i^t : 1 if flight i is the last flight performed by aircraft t, $i \in F,\ t \in T,$ and 0 o.w.

We formulate the problem as a bi-criteria nonlinear mixed-integer mathematical model with chance constraints as follows:

$$\min \quad F_1: \quad \sum_{i\in F}\sum_{t\in T}(c_{fuel}+c_{CO_2})\cdot F_i^t(f_i^t)+\sum_{i\in F}\sum_{t\in T}s_i^t\cdot Idle_t + \sum_{i\in F}\sum_{t\in T}(y_i^t+\sum_{j\in US^i}x_{ij}^t)\cdot Cspl_i\cdot\max\{0,\ Dem_i-Cap_t\} \tag{1}$$

$$\min \quad F_2: \quad \frac{1}{|T|}\sum_{t\in T}\left|\mathbb{V}^t-\bar{\mathbb{V}}\right| \tag{2}$$

$$\text{s.t.} \quad \sum_{j\in US^i}x_{ji}^t+y_i^t-\sum_{j\in DS^i}x_{ij}^t-z_i^t=0 \qquad \forall i\in F,\ t\in T \tag{3}$$

$$\sum_{i\in F}y_i^t\le 1 \qquad \forall t\in T \tag{4}$$

$$\sum_{t\in T}(y_i^t+\sum_{j\in US^i}x_{ij}^t)=1 \qquad \forall i\in F \tag{5}$$

$$\sum_{i\in F}f_i^t\le\lambda_t \qquad \forall t\in T \tag{6}$$

IF $\sum_{t\in T}x_{ij}^t=1$ THEN

$$\mathbb{P}\{NC_i\le q_i-\sum_{t\in T}(f_i^t+s_i^t)-TA_{ij}\}\ge\gamma_i \qquad \forall(i,j)\in A \tag{7}$$

$$q_i=d_j-d_i \qquad \forall(i,j)\in A \tag{8}$$

IF $(y_i^t+\sum_{j\in US^i}x_{ji}^t)=1$ THEN

$$f_i^l\le f_i^t\le f_i^u \qquad \forall i\in F,\ t\in T \tag{9}$$

ELSE

$$f_i^t=0 \quad \text{and} \quad s_i^t=0 \qquad \forall i\in F,\ t\in T \tag{10}$$

$$d_i^l\le d_i\le d_i^u \qquad \forall i\in F \tag{11}$$

$$y_i^t=0 \qquad \forall t\in T,\ i\in F\backslash F_s^t \tag{12}$$

$$z_i^t=0 \qquad \forall t\in T,\ i\in F\backslash F_e^t \tag{13}$$

$$q_i\ge 0 \qquad \forall i\in F \tag{14}$$

$$s_i^t\ge 0 \qquad \forall i\in F,\ t\in T \tag{15}$$

$$x_{ij}^t\in\{0,1\} \qquad \forall(i,j)\in A,\ t\in T \tag{16}$$

$$y_i^t\in\{0,1\} \quad \text{and} \quad z_i^t\in\{0,1\} \qquad \forall i\in F,\ t\in T \tag{17}$$

The first objective function (1) is the operational cost which is the sum of the fuel consumption and CO_2 emission costs, the idle time cost of the aircraft and the opportunity cost of spilled passengers. The second objective function (2) is the total absolute deviation of the aircraft path variabilities from the average variability. Constraints (3) are the network balance constraints. Constraints (4) ensure that each aircraft can be used for at most one path. Constraints (5) ensure that each flight can be performed by exactly one aircraft. Constraints (6) limit the total time spent by an aircraft on air in a day. The chance constraints (7) require that if two flights are performed by the same aircraft, then the probability of the non-cruise time of the earlier flight being less than or equal to the difference of departure times minus the sum of the cruise, idle, and the aircraft turnaround times should be at least the desired service level γ_i. Constraints (8) ensure that the block times of two flights that are performed by the same aircraft equals to the difference between their departure times. If flight i is performed by aircraft t then constraints (9)–(10) limit cruise time change; cruise time of a flight cannot exceed the upper and lower bounds, else the corresponding variables f_i^t and s_i^t are set to zero. Constraints (11) put lower and upper bounds on the flight departure times due to the marketing considerations. Constraints (12) and (13) sustain a maintenance policy by preventing some flights from being the first or the last flight that is operated in a day. In the current study, we limit our domain to a single day scheduling problem, although it can be extended to multi-day scheduling problem. In this case, we could use the decision variables y_i^t and z_i^t, e.g., denoting the first and last flights performed by aircraft t, respectively, along with the additional constraints to ensure the continuity between the days at each airport. Constraints (14)–(17) are non-negativity and integrality constraints.

In this formulation, the random variable NC_i denotes the non-cruise time of flight $i\in F$. According to the study of Deshpande and Arıkan (2012), non-cruise times fit a symmetric Log-Laplace distribution. Therefore, NC_i's are assumed to have Log-Laplace distribution where each random variable is associated with two parameters, α for scale and $\beta_i>0$ for shape. Then, e^{α} is the scale

Table 1
Description of the variables.

Variable	Description
ORIGIN	Origin Airport
DEST	Destination Airport
TAIL_NUM	Tail Number
CRS_DEP_TIME	Planned Departure Time (in local time: hhmm)
CRS_ARR_TIME	Planned Arrival Time (in local time: hhmm)
DEP_TIME	Actual Departure Time (in local time: hhmm)
ARR_TIME	Actual Arrival Time (in local time: hhmm)
DEP_DEL15	Departure Delay Indicator: 15 Minutes or More (1 = Yes)
ARR_DEL15	Arrival Delay Indicator: 15 Minutes or More (1 = Yes)
DEP_DEL_NEW	Difference in minutes between scheduled and actual departure time
ARR_DEL_NEW	Difference in minutes between scheduled and actual arrival time
TAXI_OUT	Taxi Out Time, in Minutes
TAXI_IN	Taxi In Time, in Minutes
AIR_TIME	Flight Time, in Minutes
DISTANCE	Distance between Airports in Miles

parameter and $1/\beta_i$ is the tail parameter. Probability density functions of NC_i is given as:

$$f_{NC_i}(\eta) = \begin{cases} \frac{1}{2\beta_i \eta} e^{\frac{\ln(\eta)-\alpha}{\beta_i}}, & \text{if } \ln(\eta) < \alpha \\ \frac{1}{2\beta_i \eta} e^{\frac{-\ln(\eta)+\alpha}{\beta_i}}, & \text{if } \ln(\eta) \geq \alpha. \end{cases} \tag{18}$$

In order to solve the proposed formulation by a commercial solver, the probabilistic chance constraints (7) can be written as

$$d_j - d_i - \sum_{t \in T} (f_i^t + s_i^t) - TA_{ij} \geq \text{VaR}_{1-\gamma_i}(NC_i) \tag{19}$$

where $\text{VaR}_{1-\gamma_i}(NC_i)$ represents the value-at-risk at the service level γ_i and it is calculated as

$$\text{VaR}_{1-\gamma_i}(NC_i) = \begin{cases} (2\gamma_i)^{\beta_i} e^{\alpha}, & \text{if } \ln(\eta) < \alpha \\ \frac{e^{\alpha}}{(2-2\gamma_i)^{\beta_i}}, & \text{if } \ln(\eta) \geq \alpha \end{cases} \tag{20}$$

where the parameter β_i is calculated as $\beta_i = \beta(e_{O_i})^2(e_{D_i})^2$ in which β is the base shape parameter and e_{O_i} and e_{D_i} represent the congestion coefficients of origin and destination airports of flight i, respectively. By replacing constraints (7) with inequality (19) in the mathematical model, chance constraints are handled via the closed-form representation of the quantile function of Log-Laplace probability distribution.

Airport congestion coefficients are calculated based on the following data-driven methodology. Intuitively, departure and arrival delay probabilities of flights, and turnaround times of the aircraft are closely related to the congestion levels in airports. Therefore, we aim to first estimate these probabilities using the historical Airline On-Time Performance Data provided by Bureau of Transportation Statistics (2021) on each flight operated between major airports in the United Stated by United Airlines in the years 2018 and 2019. The data set contains origin and destination airports of flights, tail numbers of the aircraft that operate these flights, scheduled and actual arrival and departure times, arrival and departure delays, taxi-in and taxi-out times, air times and distances of the flights. Tail numbers uniquely identify the aircraft but having only the tail number does not give further information on the type of the aircraft and its characteristics. Thus, Aircraft Registry Database of U.S. Department of Transportation (2021) is used to obtain aircraft specific information of the United States. Data set consists of 269,349 observations, one for each flight flown, across two years covering 21 major U.S. airports. Description of the variables can be found in Table 1.

Delay probabilities of flights are heavily affected by the propagation patterns as suggested by Lambelho et al. (2020). To capture these propagation effects, position of a flight in the path of an aircraft is considered in their study. We consider using the flight departure time as a surrogate measure to position of a flight. Indeed, the existing literature provides some studies which take flight departure times into account when estimating the required parameters. According to Deshpande and Arıkan (2012), airline schedule planners tend to schedule larger number of flights in the interval of 5 P.M.–6 P.M. to capture the business travel demand. Arora and Mathur (2020) suggest that afternoon and evening flights are more likely to depart late. These studies clearly indicate that the flight departure times are affecting the congestion levels in the airports and consecutively the delay probabilities significantly. In order to use departure time of a flights as a factor in our estimation models, we convert it into a categorical variable based on the segmentation based on the time intervals that the flights departure times lie in proposed by Şafak et al. (2018) with the addition of the segment IV to satisfy completeness as shown in Table 2. Therefore, the departure time of flights are used in all of the estimation models as a factor with four levels. On the other hand, Prakash (2020) assumes that the planned arrival time of a flight also has an effect on the probability of having a delayed arrival. In our proposed mathematical models, we capture the effect of arrival time on the delay probabilities of flights by approximating it with the addition of the air time of flights to their departure times. Therefore, we take flight departure times as factors that affect the estimates of departure and arrival delay probabilities of flights.

Many studies in the literature consider logit models to explain the impact of variables on on-time performance of flight schedules. In this study, two logistic regression models are constructed to estimate the departure and arrival delay probabilities. To estimate

Table 2
Segmentation for the departure time of flights.

Segment	Time Interval
I	06:00 A.M.–08:59 A.M. and after 05:00 P.M.
II	09:00 A.M.–11:59 A.M. and 03:00 P.M.–04:59 P.M.
III	12:00 noon–02:59 P.M.
IV	Before 06:00 A.M.

the departure delay probability of flight i, denoted as $p_i^{dep} \in (0,1)$, the origin airport of the flight and the time segment that the departure time of the flight lies in are determined to be the variables denoted as $x_{i,origin}$ and $x_{i,deptime}$. Then, the linear predictor $\zeta_i \in \mathbb{R}$ is constructed by

$$\zeta_i = \theta_0 + \theta_{origin} x_{i,origin} + \theta_{deptime} x_{i,deptime} \tag{21}$$

where θ_0, θ_{origin}, and $\theta_{deptime}$ are the corresponding coefficients. Finally, through the use of the logit link function, p_i^{dep} is calculated by the following characterization in Faraway (2016):

$$\zeta_i = \log\left(\frac{p_i^{dep}}{1-p_i^{dep}}\right). \tag{22}$$

A similar logistic regression model is constructed for estimating the arrival delay probabilities, denoted as $p_i^{arr} \in (0,1)$ for flight i, where the variable $x_{i,origin}$ is changed to $x_{i,destination}$ to capture the effect of the destination airport of a flight on the arrival delays.

After the departure and arrival delay probabilities are estimated, the airport congestion coefficients for flight $i \in F$ are calculated as follows:

$$e_{O_i} = (1+p_i^{dep})^2,\ e_{D_i} = (1+p_i^{arr})^2. \tag{23}$$

In addition, for each possible consecutive flight pair $(i,j) \in A$, the turnaround time TA_{ij} to prepare the aircraft between flights i and j is estimated by linear regression as follows:

$$TA_{ij} = \mu_0 + \mu_{origin} x_{j,origin} \tag{24}$$

where μ_{origin} is the corresponding coefficient to the variable $x_{j,origin}$ denoting the airport that the aircraft spends its preparation time between the flights.

A recent study by Prakash (2020) presents algorithms to determine the most reliable routes on stochastic and time-dependent networks, where the measure of reliability is defined as the probability of on-time arrival at the destination, given a threshold arrival-time. In our study, we have used the probabilistic chance constraints given as constraints (7) in the proposed formulation such that if two flights are performed by the same aircraft, then the probability of the non-cruise time of the earlier flight being less than or equal to the difference of departure times minus the sum of the cruise, idle, and the aircraft turnaround times should be at least the desired service level γ_i. Moreover, in order to solve the proposed formulation by a commercial solver, we utilize value-at-risk risk measure to reformulate the probabilistic chance constraints (7) as discussed above, and the required airport congestion coefficients in the new proposed inequality (19) are calculated based on a data-driven methodology, since departure and arrival delay probabilities of flights, and turnaround times of the aircraft are closely related to the congestion levels in airports.

In the objective function (2), the aircraft path variability of aircraft t denoted by $\mathbb{V}^t$ is calculated as $\sum_{i\in F} \mathcal{V}_i^t(O_i, D_i, d_i, f_i^t)$ where the variability of a flight leg i is calculated as

$$\mathcal{V}_i^t(O_i, D_i, d_i, f_i^t) = \begin{cases} bf_t \cdot Var(NC_i) & \text{if flight } i \text{ is operated by aircraft } t \\ 0 & \text{otherwise.} \end{cases} \tag{25}$$

Note that bf_t denotes the base value for aircraft t which is calculated by normalizing the base turntime of different aircraft provided by EUROCONTROL (2012) and $Var(NC_i)$ denotes the variance value of the Log-Laplace random variable corresponding to the non-cruise time of flight leg i as follows:

$$Var(NC_i) = e^{2\alpha}\left(\frac{1}{(\alpha-2)(\beta_i+2)} - \left[\frac{1}{(\alpha-1)(\beta_i+1)}\right]^2\right). \tag{26}$$

Furthermore, $\bar{\mathbb{V}}$ denotes the arithmetic mean of the aircraft path variabilities $\mathbb{V}^t$ over all $t \in T$ which allows us to calculate the total absolute deviation of the aircraft path variabilities from the average variability. This creates a nonlinearity due to the use of absolute value and it can be linearized by using the following set of inequalities:

$$\min \quad F_2 : \quad \frac{1}{|T|}\sum_{t\in T} v^t$$

$$\text{s.t.} \quad v^t \geq \mathbb{V}^t - \bar{\mathbb{V}} \qquad \forall t \in T \tag{27}$$

$$v^t \geq \bar{\mathbb{V}} - \mathbb{V}^t \qquad \forall t \in T \tag{28}$$

The other nonlinearity of the model stems from the objective function (1). In the objective, for flight $i \in F$ and aircraft $t \in T$, the fuel consumption function $F_i^t(f_i^t)$ is represented as

$$F_i^t(f_i^t) = \begin{cases} \left(c_1^{it} \frac{1}{f_i^t} + c_2^{it} \frac{1}{(f_i^t)^2} + c_3^{it}(f_i^t)^3 + c_4^{it}(f_i^t)^2 \right) & \text{if } y_i^t + \sum_{j \in US^i} x_{ji}^t = 1 \\ 0 & \text{if } y_i^t + \sum_{j \in US^i} x_{ji}^t = 0 \end{cases} \tag{29}$$

where f_i^t denotes the cruise time of flight i operated by aircraft t. The parameters that are required to calculate the fuel consumption can be found in EUROCONTROL (2012).

For flight $i \in F$ and aircraft $t \in T$, $F_i^t(f_i^t)$ is discontinuous and its epigraph $E_F = \{(f_i^t, \tau) \in \mathbb{R}^2 : F_i^t(f_i^t) \le \tau\}$ is nonconvex. We could obtain the convexity of E_F in the constraint set as follows:

$$\tau \ge (c_{fuel} + c_{CO_2}) \cdot (c_1^{it}\kappa_i^t + c_2^{it}\delta_i^t + c_3^{it}\phi_i^t + c_4^{it}\vartheta_i^t) \tag{30}$$

$$(y_i^t + \sum_{j \in US^i} x_{ji}^t)^2 \le \kappa_i^t \cdot f_i^t \tag{31}$$

$$(y_i^t + \sum_{j \in US^i} x_{ji}^t)^4 \le (f_i^t)^2 \cdot \delta_i^t \cdot 1 \tag{32}$$

$$(f_i^t)^4 \le (y_i^t + \sum_{j \in US^i} x_{ji}^t)^2 \cdot \phi_i^t \cdot f_i^t \tag{33}$$

$$(f_i^t)^2 \le \vartheta_i^t \cdot (y_i^t + \sum_{j \in US^i} x_{ji}^t) \tag{34}$$

Consequently, each inequality (31)–(34) can be represented by a conic quadratic inequality. Therefore, the mathematical model can be reformulated as a second order cone programming (SOCP) problem by using the conic representation of the fuel consumption function. Moreover, we implement the ε-constraint approach as discussed in T'kindt and Billaut (2006) to solve the proposed bi-criteria nonlinear mixed-integer programming problem via a commercial solver. The ε-constraint approach is frequently used in the literature since it provides the decision maker with flexibility to modify bounds on one objective to analyze the changes on the other. Therefore, we propose the following ε-constraint mathematical model denoted as (ε-CM) by bounding the operational cost by ε, e.g., constraint (35), to analyze its effects on the total deviation of aircraft path variabilities.

(ε-CM) $\min \ \frac{1}{|T|} \sum_{t \in T} \nu^t$

s.t. (3)–(17), (27)–(28), and (31)–(34),

$$\sum_{i \in F} \sum_{t \in T} (c_{fuel} + c_{CO_2}) \cdot (c_1^{it}\kappa_i^t + c_2^{it}\delta_i^t + c_3^{it}\phi_i^t + c_4^{it}\vartheta_i^t) + \sum_{i \in F} \sum_{t \in T} s_i^t \cdot Idle_t + \sum_{i \in F} \sum_{t \in T} (y_i^t + \sum_{j \in US^i} x_{ij}^t) \cdot Cspl_i \cdot \max\{0,\ Dem_i - Cap_t\} \le \varepsilon \tag{35}$$

4. Discretized approximation and aircraft swapping algorithm

To be able to solve the problem for large-sized instances, we devise a math-heuristic algorithm called discretized approximation and aircraft swapping algorithm. The main idea of the algorithm is to solve Discretized Approximation Model (DAM) first to get an initial feasible solution for aircraft routing and fleeting and then to solve the cruise speed control model (CSCM) proposed by Duran et al. (2015) to obtain the minimum cost schedule. Afterwards, Aircraft Swapping and Search Algorithm (ASSA) is applied in order to decrease the deviation of the aircraft path variability's from the average without exceeding the upper limit for the total operational cost. Flow chart of the proposed algorithm can be found in Fig. 1.

4.1. Discretized approximation model

In our proposed mathematical model, complexity of the formulation is heavily due to the SOCP-representable fuel consumption and CO_2 emission functions. Therefore, in order to solve the problem within reasonable solution times, we first use the discretized approximation model (DAM) proposed by Gürkan et al. (2016) where the cruise times of flights can only take discrete values from a pre-determined set instead of continuous values from a range. The following parameters are introduced:

crs_{ik}^t : the kth cruise time option of flight $i \in F$ operated by aircraft $t \in T$, $k \in K$

$cost_{ik}^t$: the cost of crs_{ik}^t which is equal to $(c_{fuel} + c_{CO_2}) \cdot F(crs_{ik}^t)$

Furthermore, the following binary variable is defined for each flight $i \in F$, aircraft $t \in T$, and cruise time option $k \in K$:

σ_{ik}^t : 1 if cruise time of flight i takes the kth value for aircraft t, and 0 o.w.

The formulation of DAM is as follows:

$$\min \ \sum_{t \in T} \sum_{i \in F} \sum_{k \in K} \sigma_{ik}^t \cdot cost_{ik}^t + \sum_{t \in T} \sum_{i \in F} s_i^t \cdot Idle_t + \sum_{i \in F} \sum_{t \in T} (y_i^t + \sum_{j \in US^i} x_{ij}^t) \cdot Cspl_i \cdot \max\{0,\ Dem_i - Cap_t\} \tag{36}$$

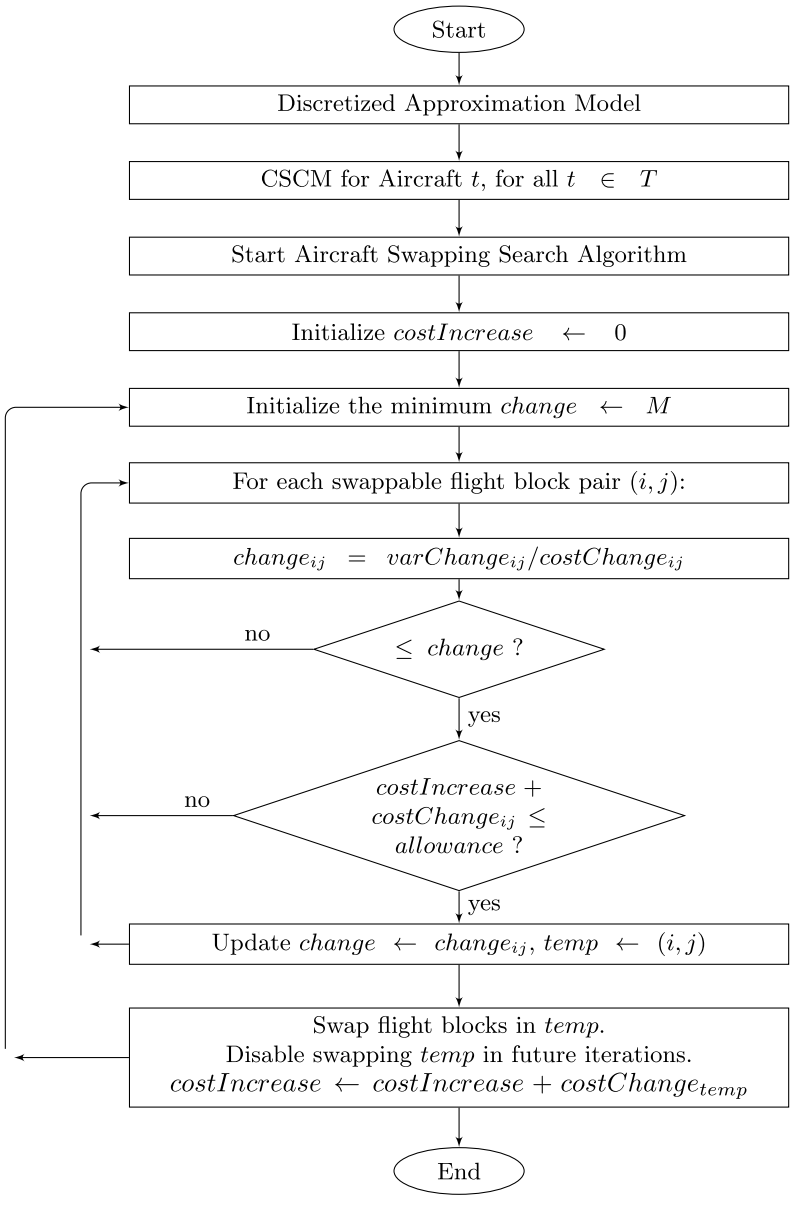

Fig. 1. Flow chart of the proposed algorithm.

s.t. (3)–(17)

$$\sum_{k \in K} \sigma_{ik}^t = (y_i^t + \sum_{j \in U S^i} x_{ji}^t) \qquad \forall i \in F,\ t \in T \tag{37}$$

$$\sum_{k \in K} \sigma_{ik}^t \cdot crs_{ik}^t = f_i^t \qquad \forall i \in F,\ t \in T \tag{38}$$

$$\sigma_{ik}^t \in \{0, 1\} \qquad \forall i \in F,\ t \in T,\ k \in K \tag{39}$$

4.2. Cruise speed control model

We could solve the DAM in a reasonable computation time, and it gives an initial feasible solution to aircraft routing, fleet assignment and schedule generation without any consideration of variability terms. However, since we have discretized cruise time in DAM, there is still a chance to improve that solution by considering a continuous value of cruise time. Therefore, after fixing fleeting and routing decisions with DAM, in order to decide continuous values of cruise time, we solve the following cruise speed

Table 3
Aircraft parameters.

Aircraft Type	B737 500	MD 83	A320 111	A320 212	B767 300	B727 228
Seat Capacity	122	148	172	180	218	134
Mass (kg)	50000	61200	62000	64000	135000	74000
Surface (m^2)	105.4	118	122.4	122.6	283.3	157.9
$C_{D0,CR}$	0.018	0.0211	0.024	0.024	0.021	0.018
$C_{D2,CR}$	0.055	0.0468	0.0375	0.0375	0.049	0.06
C_{f1}	0.46	0.7462	0.94	0.94	0.763	0.53178
C_{f2}	300	638.59	50000	100000	1430	276.72
C_{fcr}	1.079	0.9505	1.095	1.06	1.0347	0.954
MRC speed	859.2	867.6	855.15	868.79	876.70	867.6
Idle Time Cost ($)	140	142	136	144	147	150
Base Value	1.90	1.65	1.70	1.75	2.00	1.80

control model (hereafter CSCM). CSCM is a nonlinear second order cone programming model that focuses on departure timing, cruise time control and idle time insertion decisions for each path independently to obtain the minimum cost schedule. In the objective function of CSCM, the costs of fuel consumption, CO_2 emission and idle time insertion are minimized. Since the fleeting and routing decisions are already fixed by DAM, CSCM only deals with continuous decision variables. Therefore, even if it is a nonlinear model it can still be solved faster than the integrated model.

In order to use the fleeting and routing decisions obtained by DAM in the Cruise Speed Control Model (CSCM), the following notation is introduced:

$\bar{w}_i^t$: 1 if flight i is performed by aircraft t in the solution of DAM

$\bar{A}$: Set of consecutive flight pairs (i, j) performed by the same aircraft in DAM

The formulation of CSCM is as follows:

$$\min \quad \sum_{i\in F}\sum_{t\in T} \bar{w}_i^t \cdot \left(\left(c_{fuel} + c_{\mathrm{CO}_2}\right) \cdot F\left(f_i^t\right) + s_i^t \cdot Idle_t\right)$$

$$\text{s.t.} \quad d_j - d_i - \sum_{t\in T} \bar{w}_i^t (f_i^t + s_i^t) - TA_{ij} \geq \mathrm{VaR}_{1-\gamma_i}(NC_i) \qquad \forall (i,j) \in \bar{A}$$

$$f_i^l \cdot \bar{w}_i^t \leq f_i^t \leq f_i^u \cdot \bar{w}_i^t \qquad \forall i \in F, t \in T$$

$$s_i^t \leq M \cdot \bar{w}_i^t \qquad \forall i \in F, t \in T$$

(6), (11), (15)

Therefore, we solve DAM and CSCM models sequentially as shown in Fig. 1. We initially solve the DAM and fix the fleeting and routing decisions, then we solve the CSCM in order to find the minimum sum of idle time, fuel consumption and CO_2 emission costs, e.g. corresponding cruise time and idle time, if any, for a given fleeting and routing decision. In this way, instead of solving the integrated model, which is a nonlinear MIP model; as a heuristic method we propose to solve first a MIP model, e.g., DAM, and then a nonlinear model, CSCM, so that total solution time is quite smaller than the integrated model as discussed earlier.

4.3. Aircraft swapping search algorithm

Since we did not consider the aircraft path variability's in the first step, a search algorithm is proposed in order to decrease the deviation of aircraft path variability's from the average variability by swapping the aircraft. Let E denote the set of flight blocks and S be the set of flight block pairs whose operating aircraft can be swapped. The set S is generated by comparing the block times of two flight blocks and the idle time contained in them. If the block times can be arranged by adjusting the idle time and cruise times of the flights so that a flight block fits to the time interval which the other flight block occupies in the path of the aircraft, then the operating aircraft can be swapped. Then, the new set of parameters and decision variables are introduced as follows:

$minCost$: the minimum cost value of the schedule

ϱ : the percentage allowance for the cost increase

$blockVar_i^t$: variability of block i if it is operated by aircraft t, $i \in E,\ t \in T$

$pathVar^t$: variability over the path of aircraft t, $t \in T$

$aircraft^i$: aircraft assignment of flight block i, $i \in E$

a_{ij} : 1 if $(i, j) \in S$, and 0 o.w.

w_i^t : 1 if block i is performed by aircraft t, $i \in E,\ t \in T$, and 0 o.w.

u_{ij} : 1 if block i is swapped with flight block j, $(i, j) \in S$, and 0 o.w.

The idea of the search algorithm is to decide on the flight blocks whose aircraft assignments are swapped in order to have the maximum amount of decrease in the deviation of the aircraft path variabilities from the average while satisfying the upper limit for

the total operational cost. To be able to achieve that, the swap which gives the maximum decrease in the deviation of variabilities with the minimum increase in the total operational cost is selected in a knapsack framework. The pseudo-code can be found in Algorithm 1.

Algorithm 1 Aircraft Swapping Search Algorithm.

Initialize: $costOfSchedule \leftarrow minCost$
Set: $maxCost \leftarrow minCost \times (1+\rho)$
for each $t \in T$ **do**
  for each $j \in \{0,\dots,|E|\}$ **do**
    $pathVar^t \leftarrow pathVar^t + w_j^t \cdot blockVar_j^t$ ▷ Calculate path variabilities.
  end for
end for
for each $j \in \{0,\dots,|E|\}$ **do**
  for each $k \in \{0,\dots,|E|\}$ **do**
    $varChange_{jk} \leftarrow$ change in the absolute deviation of path variabilities from average if flight block j is swapped with k.
    $costChange_{jk} \leftarrow$ increase in the total operational cost if flight block j is swapped with k.
  end for
  $k^\star \leftarrow \arg\min_{k\in\{0,\dots,|E|\}\ :\ aircraft^j \neq aircraft^k,\ a_{jk}=1} \{\frac{varChange_{jk}}{costChange_{jk}}\}$
  if $varChange_{jk^\star} \leq 0$ **and** $costOfSchedule + costChange_{jk^\star} \leq maxCost$ **then**
    $w_j^{aircraft^j} \leftarrow 0$ and $w_{k^\star}^{aircraft^{k^\star}} \leftarrow 0$ ▷ Remove initial aircraft assignments.
    $aircraft^j \leftrightarrow aircraft^{k^\star}$ ▷ Swap the aircraft assignments.
    $u_{jk^\star} \leftarrow 1$ ▷ Swap flight blocks j and $k^\star$.
    $w_j^{aircraft^j} \leftarrow 1$ and $w_{k^\star}^{aircraft^{k^\star}} \leftarrow 1$ ▷ Reassign aircraft to flight blocks j, $k^\star$.
    $costOfSchedule \leftarrow costOfSchedule + costChange_{jk^\star}$ ▷ Update the cost.
  end if
  Re-calculate path variabilities $pathVar^t$ for all $t \in T$ (same as in steps 2-6).
end for

5. Computational study

In order to obtain sample schedules and generate flight and aircraft sets, we used "Airline On-Time Performance" database of Bureau of Transportation Statistics (2021). In all of the subsets of the flight legs that we select, Chicago O'Hare International Airport (ORD) serves as the hub airport. This means that all the available aircraft have to depart first from ORD in the beginning of the daily planning horizon. We consider six different types of aircraft with different parameters as presented in EUROCONTROL (2012). Seat capacity, mass, wing surface area, fuel consumption coefficients, maximum range cruise (MRC) speed, idle time cost and base value parameters are available in Table 3. In our computational experiments, we initially assume unit cost of fuel consumption as $c_{fuel} = 1.2$ \$/kg and unit cost of CO_2 emission as $c_{CO_2} = 0.02$ \$/kg. In addition, we initially take $\beta = 0.01$, which is the base shape parameter of the Log-Laplace random variables denoting the non-cruise times, to calculate the tail parameter β_i for each flight i. Also, the scale parameter α is adjusted as $e^\alpha = 20$ to have non-cruise times which are deviating from 20 min. Afterwards, in Section 6, we will evaluate different experimental settings.

All computational experiments are conducted on an AMD Ryzen 7 5800X 8-core 16-thread computer with 3.8 GHz processor and 32 GB RAM. The problem is implemented in Java programming language with a connection to IBM ILOG CPLEX Optimization Studio 20.1.0.

5.1. Estimation of airport congestion coefficients

As expected, not all airports have the same level of congestion due to geographical reasons. Intuitively, one can expect the hubs to be more congested. Since the level of congestion differs in the airports, we assume departure and arrival delays occurred in different origin and destination airports have different means and variances which have effects on the on-time probabilities. Similarly, flight departure time has also an effect on the turnaround time required to prepare the aircraft between two flights. Therefore, in our proposed models, origin and destination airports of flights are taken as factors to estimate both departure and arrival delays, and also turnaround times. In short, we consider flight departure times, origin and destination airports as the factors that affect our estimation of the related response variables.

Using logistic regression models as discussed in Section 3, departure and arrival delay probabilities for 269,349 flights operated by United Airlines across 21 major U.S. airports are estimated. Afterwards, the departure and arrival congestion coefficients are calculated based on the delay probabilities, separately. We distinguish the departure and arrival delay probabilities of a flight from each other to see the effects of this difference on the congestion coefficients of airports. As it can be seen from the Table 4, for a given airport, departure and arrival congestion coefficients are different. For example, departure congestion coefficient of FLL (Fort Lauderdale-Hollywood Intl. Airport) is up to 1.225 whereas arrival congestion coefficient of FLL is up to 1.553. In the existing literature, it was assumed that for a flight, having a particular airport as either its origin or destination airport has the same effect on its congestion level. By distinguishing the departure and arrival delay probabilities, we are able to capture the effects of the different congestion levels of origin and destination airports of flights.

Table 4
Departure and arrival congestion coefficients of 21 major U.S. airports in four time segments.

Departure Congestion Coefficient				
Airport	Time Segment			
	I	II	III	IV
ATL	1.304	1.311	1.350	1.051
AUS	1.164	1.169	1.190	1.026
BOS	1.214	1.219	1.245	1.034
DCA	1.147	1.151	1.171	1.024
DEN	1.217	1.221	1.250	1.036
DFW	1.232	1.237	1.266	1.038
EWR	1.320	1.327	1.367	1.053
FLL	1.197	1.201	1.225	1.032
LAS	1.186	1.190	1.214	1.030
LAX	1.162	1.166	1.188	1.026
LGA	1.201	1.208	1.232	1.032
MCI	1.117	1.119	1.136	1.018
MIA	1.221	1.228	1.254	1.036
MSP	1.175	1.177	1.201	1.028
ORD	1.261	1.266	1.300	1.042
PHL	1.199	1.203	1.230	1.032
PHX	1.190	1.197	1.221	1.030
SAN	1.175	1.179	1.201	1.028
SFO	1.266	1.272	1.304	1.044
SLC	1.320	1.327	1.367	1.055
STL	1.241	1.248	1.277	1.040
Arrival Congestion Coefficient				
Airport	Time Segment			
	I	II	III	IV
ATL	1.378	1.234	1.243	1.277
AUS	1.369	1.228	1.239	1.270
BOS	1.397	1.245	1.257	1.290
DCA	1.383	1.237	1.248	1.279
DEN	1.318	1.195	1.203	1.230
DFW	1.498	1.313	1.327	1.369
EWR	1.395	1.243	1.254	1.288
FLL	1.553	1.350	1.364	1.409
LAS	1.360	1.221	1.232	1.261
LAX	1.350	1.217	1.225	1.254
LGA	1.440	1.275	1.286	1.323
MCI	1.414	1.257	1.268	1.304
MIA	1.476	1.297	1.311	1.350
MSP	1.381	1.237	1.245	1.277
ORD	1.339	1.208	1.217	1.245
PHL	1.397	1.245	1.257	1.290
PHX	1.395	1.243	1.254	1.300
SAN	1.357	1.221	1.230	1.254
SFO	1.383	1.237	1.248	1.279
SLC	1.397	1.245	1.257	1.290
STL	1.332	1.203	1.212	1.241

An important observation, the earlier studies estimated the airport congestion coefficients based on the number of passengers visiting a particular airport provided in T-100 Domestic Market Data of Bureau of Transportation Statistics (2020) regardless of departure or arrival events, that may not be a realistic representation as can be seen from Table 4. For example, MIA (Miami Intl. Airport) has the highest number passengers and consequently assigned the largest airport congestion coefficient in earlier studies, followed by ORD (Chicago O'Hare Intl. Airport), DEN (Denver Intl. Airport) and DFW (Dallas/Fort Worth Intl. Airport). In contrary, DEN has one of the lowest arrival delay occurrence and consequently one of the lowest arrival congestion coefficients according to our data analysis. Besides the delay probabilities, base turnaround times needed to prepare the aircraft between consecutive flights in 21 different airports are estimated by a linear regression model.

5.2. Computational analysis on the schedule with 50 flights

We first analyzed the flight network containing 50 flights operated by 10 aircraft in detail. The corresponding minimum cost schedule $\mathcal{P}_1$ and the proposed bi-criteria schedule $\mathcal{P}_2$ are given in Table 5. To obtain $\mathcal{P}_2$, the allowance for the cost increase is set to 10% of the total operational cost of $\mathcal{P}_1$ for the ASSA.

Table 5
Schedules for the 50 Flight Network.

Tail No.	Aircraft No.	Minimum Cost Schedule $\mathcal{P}_1$					Proposed Schedule $\mathcal{P}_2$				
		Flight No.	Origin	Dest.	Departure Time	Arrival Time	Flight No.	Origin	Dest.	Departure Time	Arrival Time
N678UA	0	0	ORD	LGA	08:10	09:52	0	ORD	LGA	08:10	09:52
		36	LGA	ORD	10:45	12:42	36	LGA	ORD	10:44	12:42
		42	ORD	LGA	14:18	16:00	42	ORD	LGA	14:17	15:59
		8	LGA	ORD	17:24	19:21	8	LGA	ORD	17:24	19:22
		19	ORD	BOS	21:30	23:14	14	ORD	DEN	21:30	23:20
N802WA	1	30	ORD	DFW	07:29	08:59	Same				
		6	DFW	ORD	10:19	11:43					
		32	ORD	AUS	13:50	15:32					
		33	AUS	ORD	17:22	18:59					
		4	ORD	LGA	20:20	22:02					
N805WA	2	5	ORD	DFW	07:45	09:15	Same				
		41	DFW	ORD	10:23	11:47					
		2	ORD	DFW	13:35	15:05					
		3	DFW	ORD	17:22	18:46					
		44	ORD	SAN	20:00	21:39					
N309US	3	15	ORD	MSP	07:15	08:19	Same				
		16	MSP	ORD	09:15	10:17					
		17	ORD	SAN	11:49	13:28					
		18	SAN	ORD	16:47	18:10					
		24	ORD	SAN	19:00	20:39					
N334NW	4	45	ORD	MCI	07:15	08:15	45	ORD	MCI	07:15	08:16
		11	MCI	ORD	09:12	10:11	11	MCI	ORD	09:12	10:11
		47	ORD	DFW	11:22	12:52	47	ORD	DFW	11:22	12:52
		48	DFW	ORD	14:35	15:59	48	DFW	ORD	14:35	15:59
		49	ORD	DEN	17:30	19:20	29	ORD	BOS	17:31	19:14
N312US	5	10	ORD	MCI	07:15	08:15	10	ORD	MCI	07:15	08:16
		46	MCI	ORD	09:12	10:11	46	MCI	ORD	09:12	10:11
		12	ORD	DFW	11:22	12:52	12	ORD	DFW	11:22	12:52
		13	DFW	ORD	14:35	15:59	13	DFW	ORD	14:35	15:59
		14	ORD	DEN	17:30	19:20	19	ORD	BOS	17:31	19:14
N681UA	6	25	ORD	DFW	08:45	10:15	27	ORD	LGA	08:45	10:27
		26	DFW	ORD	11:09	12:33	28	LGA	ORD	11:20	13:17
		7	ORD	LGA	14:18	16:00	7	ORD	LGA	16:37	18:19
		43	LGA	ORD	17:24	19:21	43	LGA	ORD	19:44	21:41
		34	ORD	LGA	20:40	22:22	34	ORD	LGA	23:00	00:42
N807TR	7	40	ORD	DFW	07:45	09:15	Same				
		31	DFW	ORD	10:29	11:53					
		37	ORD	DFW	13:35	15:05					
		38	DFW	ORD	17:22	18:46					
		39	ORD	LGA	20:20	22:02					
N695UA	8	35	ORD	LGA	08:06	09:48	35	ORD	LGA	08:07	09:49
		1	LGA	ORD	10:41	12:39	1	LGA	ORD	10:41	12:39
		27	ORD	LGA	13:33	15:15	25	ORD	DFW	13:34	15:04
		28	LGA	ORD	16:08	18:06	26	DFW	ORD	15:58	17:22
		29	ORD	BOS	19:01	20:44	49	ORD	DEN	19:17	21:07
N422BN	9	20	ORD	DFW	09:45	11:15	Same				
		21	DFW	ORD	12:34	13:58					
		22	ORD	STL	15:17	16:49					
		23	STL	ORD	17:42	19:08					
		9	ORD	SAN	20:00	21:39					

5.2.1. Posterior analysis on resilience

In order to measure and compare the resilience of the minimum cost schedule $\mathcal{P}_1$ and the proposed schedule $\mathcal{P}_2$, we generated disruption scenarios due to the unavailability of the aircraft. Initially, we consider the unavailability periods as equal to the whole day which means that in total, there are 10 disruption scenarios. In other words, we let ω_t denote that the aircraft $t = 0, \ldots, 9$ is unavailable for the whole day. Then, we applied the Integrated Flight and Passenger Recovery Algorithm, which is available in Appendix A, to observe the recovery performances. In Table 6, the recovery solutions against each disruption scenario ω_t is presented. For each scenario, there are multiple recovery solutions with different number of cancelled flights and different amounts of total delay. The recovery solutions which are presented in Table 6 are the ones with the minimum number of cancelled flights

Table 6
Recovery solutions under each disruption scenario for 50 flights.

Disruption Scenario	Min. Cost Schedule $\mathcal{P}_1$		Proposed Schedule $\mathcal{P}_2$		Change	
	# Cancelled Flights: ξ_1	Total Delay: ξ_2 (mins)	# Cancelled Flights: ξ_1	Total Delay: ξ_2 (mins)	ξ_1	ξ_2
ω_0	5	–	1	1416	−4	–
ω_1	3	891	1	1166	−2	31%
ω_2	3	990	1	1414	−2	43%
ω_3	3	905	1	925	−2	2%
ω_4	3	791	1	892	−2	13%
ω_5	3	841	1	898	−2	7%
ω_6	5	–	3	1012	−2	–
ω_7	3	847	1	1437	−2	70%
ω_8	5	–	3	1125	−2	–
ω_9	3	581	1	937	−2	61%
Average:	3.6	835	1.4	1122	−2.2	34%

for both of the schedules. If there are multiple recovery solutions with the same number of cancelled flights for a schedule, the solutions with the shortest total delay is selected.

When we categorize the disruption scenarios according to which type of recovery solution that they yield, we observed that all the scenarios except ω_0, ω_6, and ω_8 yield non-dominated recovery solutions for our proposed schedule. That means that $\mathcal{P}_2$ recovers from the disruption with less number of cancelled flights but more time of delay. It is due to the fact that disrupted flights are recovered by accommodating them into the paths of the non-disrupted aircraft, which may cause an increase in the total time of delay in order to prevent flight cancellation.

When the aircraft 1–5, 7, and 9 are disrupted, the proposed schedule is recovered by cancelling only 1 flight whereas the minimum cost schedule cancels 3 flights. This means that $\mathcal{P}_2$ performs 67% "better" than $\mathcal{P}_1$ in terms of the number of cancelled flights. However, in $\mathcal{P}_2$, there occurs 31% more time of delay on average since it accommodates more flights instead of cancelling them. Under disruption scenarios ω_0, ω_6, and ω_8, the minimum cost schedule $\mathcal{P}_1$ cancels all of the disrupted flights whereas the proposed schedule $\mathcal{P}_2$ is able to recover from the disruptions with up to 3 cancelled flights. Although cancelling all of the disrupted flights in $\mathcal{P}_1$ creates 0 delay, we classify these scenarios as yielding strongly-dominating recovery solutions.

5.3. Computational analysis on the schedule with 150 flights

In order to test our proposed methodology with a larger sized problem, the network containing 150 flights operated by 30 different aircraft is also analyzed. First, the minimum cost schedule $\mathcal{P}_1$ is generated and then, the Aircraft Swapping Search Algorithm is applied by allowing 10% increase in the total operational cost to obtain the proposed bi-criteria schedule $\mathcal{P}_2$. The resulting schedules $\mathcal{P}_1$ and $\mathcal{P}_2$ can be found in Appendix B.

The Aircraft Swapping Search algorithm achieves the proposed schedule $\mathcal{P}_2$ in 9 iterations and in each iteration, the aircraft assignments of a pair of flight blocks are swapped. The relationship between the total operational cost and the deviation of aircraft path variability's from average for the minimum cost schedule $\mathcal{P}_1$, the proposed schedule $\mathcal{P}_2$, and the schedules that are obtained in the intermediate steps of the algorithm can be seen from the Pareto frontier presented in Fig. 2.

As it can be seen in Fig. 2, when we allow the total operational cost to deviate from the minimum by at most 10%, the deviation of the aircraft path variability's from the average, i.e. F_2, decreases by 47%. Additionally, we examine different allowance values for the cost increase as in Fig. 3 and we observed that instead of 10%, if the allowance is 2.5%, 5%, and 7.5% then F_2 decreases by 23%, 30%, and 41%, respectively.

5.3.1. Posterior analysis on resilience

To measure the resilience of our proposed schedule by comparing the recovery performances of $\mathcal{P}_1$ and $\mathcal{P}_2$, a posterior analysis is conducted. For each aircraft, a disruption scenario caused by the unavailability of the aircraft for a whole day is generated. We let ω_t denote that the aircraft $t \in \{0, \dots, 29\}$ is unavailable for the day. Afterwards, for each scenario, we execute the Integrated Flight and Passenger Recovery Algorithm, and a summary of the recovery solutions for the 30 disruption scenarios is given in Table 7.

Under 22 of the 30 disruption scenarios, the proposed schedule $\mathcal{P}_2$ yields strongly-dominating recovery solutions. On the average of these 22 scenarios, $\mathcal{P}_2$ recovers from the disruption by cancelling 2.6 less flights than $\mathcal{P}_1$ which corresponds to a 68% improvement in ξ_1. Also, $\mathcal{P}_2$ recovers with an average of 825 min total delay whereas $\mathcal{P}_1$ recovers with 1002 min which corresponds to a 18% improvement in ξ_2. We interpret this result as follows. As the number of flights in the schedule increases, the number of possible recovery actions also increases. Hence, under these scenarios, the recovery algorithm is able to find strategies which are better in terms of not only one of cancellation or delay but both which is why we introduce the term strongly dominating solutions. This shows that it may not be necessary to have a strict trade-off between the number of cancelled flights and total delay in the schedules. Under the remaining 8 disruption scenarios, the proposed schedule $\mathcal{P}_2$ yields non-dominated recovery solutions. On the average of these 8 scenarios, $\mathcal{P}_2$ recovers by cancelling 2.5 less flights than $\mathcal{P}_1$ but more time of delay. It corresponds to a 68% improvement

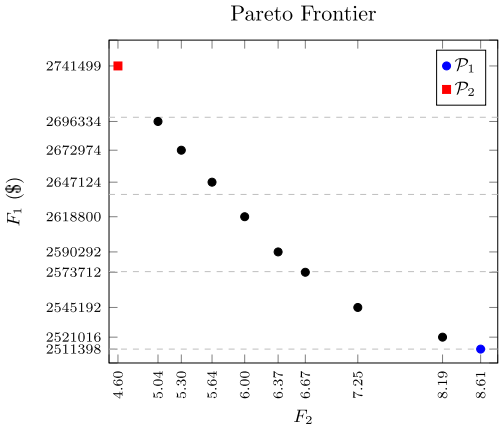

Fig. 2. Average variability vs. total operational cost for 150 flights.

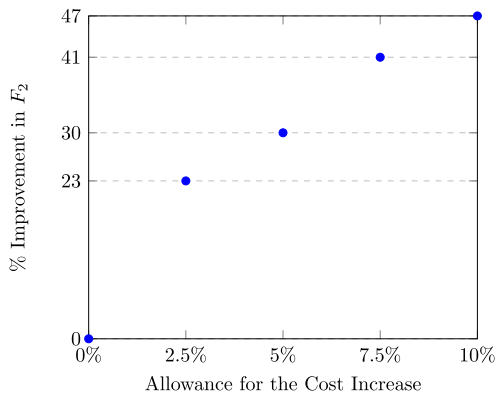

Fig. 3. Allowance for the cost increase vs. improvement in F_2 for 150 flights.

Table 7
Summary of recovery solutions for 150 flights.

Recovery Solution Type	Number of Scenarios	Performance Measures					
		ξ_1			ξ_2		
		$\mathcal{P}_1$	$\mathcal{P}_2$	Change	$\mathcal{P}_1$	$\mathcal{P}_2$	Change
Strongly-Dominating:	22	3.8	1.2	−68%	1002	825	−18%
Non-Dominated:	8	3.1	1	−68%	751	959	28%
Overall:	30	3.6	1.1	−69%	911	861	−6%

in ξ_1 whereas ξ_2 increases by 28%. Overall, the recovery performance of $\mathcal{P}_2$ is "better" than $\mathcal{P}_1$ by 69% in terms of the number of cancelled flights and 6% in terms of the total time of delay after recovery against 30 disruption scenarios. Detailed information on the recovery solutions against each of these scenarios can be found in Table 8.

6. Managerial insights

The conducted computational study intrigues various questions about the behaviour and performance of our proposed schedules. In this section, some managerial insights into the problem dynamics are given. To observe the effects of the problem parameters on the generated schedules and their recovery performances, several what if analyses are conducted where the factors such as unit fuel cost, β, α, and the allowance for the cost increase ϱ take different values as shown in Table 9. We report our analysis on unit fuel cost and ϱ below since they have a more relevant impact on the recovery performances, whereas the non-cruise time parameters β and α are given in Appendix C. In addition to the problem parameters, we have also conducted computational experiments by generating different disruption scenarios, such as the number of disrupted aircraft in a scenario, the aircraft unavailability periods, or airport closures below, and analyzed their impact on the recovery performance measures of $\mathcal{P}_1$ and $\mathcal{P}_2$.

Table 8
Recovery solutions under each disruption scenario for 150 flights.

Disruption Scenario	Min. Cost Schedule $\mathcal{P}_1$		Proposed Schedule $\mathcal{P}_2$		Change	
	# Cancelled Flights: ξ_1	Total Delay: ξ_2 (mins)	# Cancelled Flights: ξ_1	Total Delay: ξ_2 (mins)	ξ_1	ξ_2
ω_0	5	–	1	1168	−4	–
ω_1	3	869	1	709	−2	−18%
ω_2	3	1229	1	962	−2	−22%
ω_3	3	1186	1	720	−2	−39%
ω_4	3	733	1	786	−2	7%
ω_5	3	872	1	876	−2	0%
ω_6	5	–	1	1215	−4	–
ω_7	3	1358	1	905	−2	−33%
ω_8	4	–	1	1190	−4	–
ω_9	3	656	1	804	−2	23%
ω_{10}	3	1016	1	932	−3	−8%
ω_{11}	3	731	1	350	−2	−52%
ω_{12}	4	785	1	569	−2	−28%
ω_{13}	3	1006	1	1081	−2	7%
ω_{14}	5	439	1	922	−3	110%
ω_{15}	3	1000	1	1271	−2	27%
ω_{16}	5	–	1	1190	−4	–
ω_{17}	3	1068	1	800	−2	−25%
ω_{18}	5	–	3	231	−2	–
ω_{19}	3	600	1	975	−2	63%
ω_{20}	5	–	3	259	−2	–
ω_{21}	3	1107	1	1037	−2	−6%
ω_{22}	5	–	1	1151	−4	–
ω_{23}	3	1050	1	868	−2	−17%
ω_{24}	5	–	1	1190	−4	–
ω_{25}	3	617	1	503	−2	−18%
ω_{26}	3	1101	1	918	−2	−17%
ω_{27}	3	927	1	505	−2	−46%
ω_{28}	3	989	1	773	−2	−22%
ω_{29}	3	704	1	956	−2	36%
Average:	3.6	911	1.1	861	−2.5	−6%

Table 9
Factor values of problem parameters.

Factor	Levels
Unit fuel cost ($)	0.6, 1.2, 1.8
β	0.01, 0.05
α	ln(20), ln(25)
Allowance ρ	0%, 2.5%, 5%, 7.5%, 10%, 15%

Table 10
Effect of unit fuel cost on the schedule generation.

Unit Fuel Cost ($/kg)	Min. Cost Schedule $\mathcal{P}_1$		Proposed Schedule $\mathcal{P}_2$		Improvement in F_2
	F_1 ($)	F_2	F_1 ($)	F_2	
0.6	398147	6.01	422517	5.19	14%
1.2	796294	5.32	874284	3.24	39%
1.8	1194441	5.30	1276911	3.15	39%

6.1. What if analysis on fuel cost

Let the unit fuel cost and unit CO_2 emission cost be an experimental factor denoted by A. We set the fuel cost to 0.6, 1.2, and 1.8 $/kg and correspondingly, we set the CO_2 emission cost to 0.01, 0.02, and 0.03 $/kg for these settings. For each case, we first obtained the minimum cost schedules, and then, to obtain the proposed schedules we allowed a 10% increase in the total operational cost of the minimum cost schedule as presented in Table 10.

As expected, when the unit fuel consumption cost increases, the total operational cost of the schedule increases as well. As a result of that, when applying the Aircraft Swapping and Search Algorithm, if the percentage allowance for the cost increase is taken equal for each schedule, then the schedule with the highest unit fuel cost level has more allowance for making aircraft swaps. Therefore, the improvement in the deviation of aircraft path variability's is higher when the unit cost value is higher. In order to

Table 11
Effect of unit fuel cost on the recovery performance.

Disruption Scenario	Unit Fuel Cost 0.6 $/kg				Unit Fuel Cost 1.2 $/kg				Unit Fuel Cost 1.8 $/kg			
	$\mathcal{P}_1$		$\mathcal{P}_2$		$\mathcal{P}_1$		$\mathcal{P}_2$		$\mathcal{P}_1$		$\mathcal{P}_2$	
	ξ_1	ξ_2	ξ_1	ξ_2	ξ_1	ξ_2	ξ_1	ξ_2	ξ_1	ξ_2	ξ_1	ξ_2
ω_0	5	–	1	1540	5	–	1	1416	5	–	1	606
ω_1	4	660	1	1283	3	891	1	1166	3	974	1	990
ω_2	3	986	1	1300	3	990	1	1414	4	556	1	1534
ω_3	3	987	2	573	3	905	1	925	3	886	1	1026
ω_4	3	935	1	666	3	791	1	892	3	949	1	667
ω_5	3	841	1	694	3	841	1	898	3	746	1	974
ω_6	4	631	4	414	5	–	3	1012	3	886	1	583
ω_7	3	788	1	1213	3	847	1	1437	3	1225	1	1240
ω_8	5	–	1	1420	5	–	3	1125	5	–	2	1077
ω_9	3	587	1	784	3	581	1	937	3	1184	1	954
Average:	3.4	802	1.4	989	3.6	835	1.4	1122	3.5	926	1.1	965

Table 12
Minimum cost vs. proposed schedule for unit fuel cost levels.

Unit Fuel Cost ($/kg)	Change in the Recovery Performance	
	# of Cancelled Flights (ξ_1)	Total Time of Delay (ξ_2)
0.6	−59%	23%
1.2	−61%	34%
1.8	−69%	4%

Table 13
Effect of allowance for cost increase on the schedule generation.

Percentage Allowance for the Cost Increase (ϱ)	F_1 ($)	F_2	# of Swaps Made	Inserted Idle Time (mins)
0% (Min. Cost Schedule)	796294	5.32	–	0
2.5%	796294	5.32	0	0
5%	818284	4.58	1	155
7.5%	845912	3.85	2	355
10%	874284	3.24	3	555
15%	913564	2.50	4	832

find out if this has an effect on the recovery performance of the schedules, we conducted a posterior analysis whose results are shown in Table 11.

When the recovery solutions are generated against each disruption scenario, it is observed that the proposed schedule is able to recover from the disruption with less number of cancelled flights compared to the minimum cost schedule in each of the fuel cost levels. As a result of that, total delay occurring in the schedule may increase. In addition to that, under some scenarios such as ω_3 and ω_6, as the unit fuel cost increases, the number of cancelled flights after recovery in the proposed schedule $\mathcal{P}_2$ decreases. On the average, $\mathcal{P}_2$ recovers from the disruptions by 2, 2.2, and 2.4 less cancelled flights than the minimum cost schedule $\mathcal{P}_1$ in the settings 0.6, 1.2 and 1.8, respectively. Improvements observed in our recovery performance measures ξ_1 and ξ_2 can be seen from Table 12 as well, e.g., the number of cancelled flights after recovery is increased from 59% to 69% as the unit fuel cost changes from 0.6 to 1.8 $/kg. Although total time of delay is higher in the proposed schedule compared to the minimum cost schedule in each of these settings, as the unit fuel cost increases, the change in the total time of delay decreases from 23% to 4% which is acceptable considering the improvement made in the number of cancelled flights. Our results clearly indicate that the fuel cost has a significant impact on the recovery performance. For further insight, the results of the what if analysis on the percentage allowance for cost increase will be examined in Section 6.2.

6.2. What if analysis on the allowance for cost increase ϱ

In the Proposed Discretized Approximation and Aircraft Swapping Algorithm, the total operational cost of the proposed schedule is allowed to deviate from the minimum cost by at most ϱ. To observe the effects of the allowance for the cost increase on the recovery performances on the proposed schedules, ϱ is set to 2.5%, 5%, 7.5%, 10%, and 15%. The total operational cost, F_1, and the deviation of aircraft path variability's from the average, F_2, can be seen in Table 13 for each of the corresponding schedules.

When the allowance is equal to 2.5%, the algorithm cannot make any swaps for the 50-flight schedule, and returns exactly the same minimum cost schedule. However, as the percentage allowance increases, the algorithm is able to make more swaps and to insert more idle time to the schedule. Therefore, when the allowance is equal to 15%, a total of 832 min idle time is inserted into the schedule and the variability level is decreased to 2.50, which corresponds to a 56% improvement in F_2. Fig. 4 shows how the

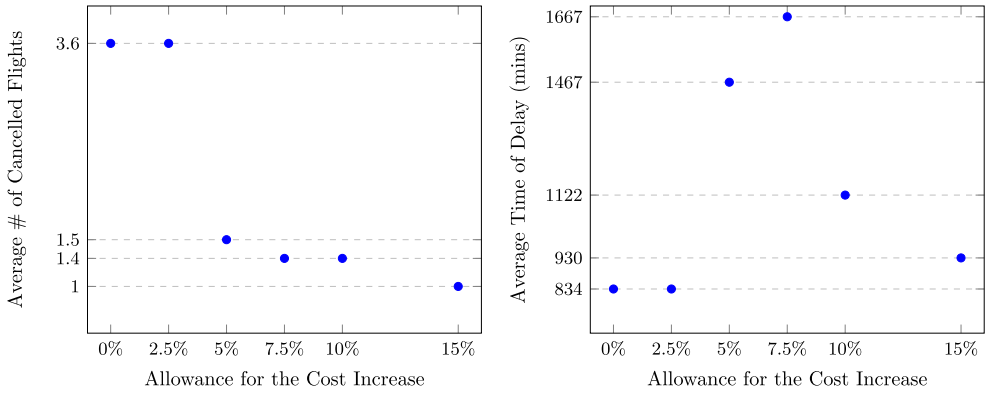

Fig. 4. Effects of allowance for cost increase on recovery performance.

Table 14
Impact of ϱ on recovery performance measures for each scenario.

Disruption Scenario	Number of Cancelled Flights (ξ_1)					Total Time of Delay (ξ_2) (mins)				
	Allowance for Cost Increase (ρ)					Allowance for Cost Increase (ρ)				
	0%–2.5%	5%	7.5%	10%	15%	0%–2.5%	5%	7.5%	10%	15%
ω_0	5	1	1	1	1	-	1438	1438	1416	1237
ω_1	3	1	1	1	1	891	1520	1441	1166	931
ω_2	3	1	1	1	1	990	1414	1414	1414	1261
ω_3	3	1	1	1	1	905	1214	925	925	925
ω_4	3	1	1	1	1	791	1161	892	892	715
ω_5	3	1	1	1	1	841	1162	892	898	715
ω_6	5	3	3	3	1	-	1012	1012	1012	834
ω_7	3	1	1	1	1	847	1436	1436	1436	1066
ω_8	5	4	3	3	1	-	173	1282	1125	942
ω_9	3	1	1	1	1	581	937	937	937	669
Average:	3.6	1.5	1.4	1.4	1	835	1467	1667	1122	930

number of cancelled flights and total time of delay occurred after recovery change when the allowance for the cost increase changes on the average. As expected, the number of cancelled flights on average decreases as ϱ increases. When we compare the cases for 5% and 7.5% allowance, the average number of cancelled flights is reduced from 1.5 to 1.4, but this results in an increase in the total delay due to accommodating more flights into the schedule. In our proposed recovery algorithm, we have used a hierarchical evaluation of two performance measures such that decreasing the number of cancellations is taken as the primary whereas reducing the total delay is considered as the secondary criterion, since the opportunity costs of flight cancellation are quite high and also the passenger convenience and satisfaction are of great importance to airlines. For the 50 flight network schedule, increasing ϱ from 7.5 to 10% results in the same cancellation performance, but with a significant decrease in total delay performance (as expected) as shown in Fig. 4, due to the fact that increasing ϱ directly corresponds to increasing operational costs, e.g., fuel consumption and idle time costs.

In addition to the changes in the average of the recovery performance measures, recovery solutions generated for each proposed schedule having different allowance values under each disruption scenario is presented in Table 14. Under each of the disruption scenarios, the number of cancelled flights either decreases or stays the same as the percentage allowance increases which is in line with our expectations. Similarly, under all disruption scenarios except ω_0, ω_6, and ω_8, total time of delay after recovery decreases as the allowance increases. Under scenarios ω_0, ω_6, and ω_8, since the schedules with lower allowance values cancel significantly more flights to recover, less times of delay occur in those schedules as expected.

6.3. What if analysis on the recovery performance measures

Although the proposed schedules are shown to perform better against disruptions in terms of the number of cancelled flights, they may have longer durations of total delay due to the higher number of flights accommodated into the existing schedule. Because of that, we also consider the maximum time of delay occurred in a single flight leg as another performance measure. Corresponding analysis for 50 flights is shown in Table 15. While on the average, the proposed schedule $\mathcal{P}_2$ has 61% less number of cancelled flights with 34% more time of total delay compared to the minimum cost schedule $\mathcal{P}_1$, when we consider the maximum time of delay occurred in a single flight leg, $\mathcal{P}_2$ has only 5% more delay than $\mathcal{P}_1$.

We also consider this performance measure for the network containing 150 flights in Table 16 on the average of 30 disruption scenarios. While decreasing the number of cancelled flights by 67%, the proposed schedule performs 6% better in terms of the total

Table 15
Comparison of total delay and maximum delay for 50 flights.

Disruption Scenario	# of Cancelled Flights			Total Time of Delay			Max. Delay in a Flight Leg		
	$\mathcal{P}_1$	$\mathcal{P}_2$	Change	$\mathcal{P}_1$	$\mathcal{P}_2$	Change	$\mathcal{P}_1$	$\mathcal{P}_2$	Change
ω_0	5	1	−80%	–	1416	–	–	262	–
ω_1	3	1	−67%	891	1166	31%	214	241	13%
ω_2	3	1	−67%	990	1414	43%	260	213	−18%
ω_3	3	1	−67%	905	925	2%	199	220	11%
ω_4	3	1	−67%	791	892	13%	256	212	−17%
ω_5	3	1	−67%	841	898	7%	213	213	0%
ω_6	5	3	−40%	–	1012	–	–	267	–
ω_7	3	1	−67%	847	1437	70%	214	259	21%
ω_8	5	3	−40%	–	1125	–	–	262	–
ω_9	3	1	−67%	581	937	61%	214	214	0%
Average:	3.6	1.4	−61%	835	1122	34%	224	236	5%

Table 16
Changes in the recovery performance measures for 150 flights.

	# of Cancelled Flights	Total Time of Delay	Max. Delay in a Flight Leg
Min. Cost Schedule $\mathcal{P}_1$	3.6	911	221
Proposed Schedule $\mathcal{P}_2$	1.1	861	210
Change:	−67%	−6%	−5%

Table 17
Comparison of total delay and maximum delay for 150 flights.

Disruption Scenario	# of Cancelled Flights			Total Time of Delay			Max. Delay in a Flight Leg		
	$\mathcal{P}_1$	$\mathcal{P}_2$	Change	$\mathcal{P}_1$	$\mathcal{P}_2$	Change	$\mathcal{P}_1$	$\mathcal{P}_2$	Change
ω_0	5	1	−80%	–	1168	–	–	212	–
ω_1	3	1	−67%	869	709	−18%	212	214	1%
ω_2	3	1	−67%	1229	962	−22%	212	149	−30%
ω_3	3	1	−67%	1186	720	−39%	253	212	−16%
ω_4	3	1	−67%	733	786	7%	213	257	21%
ω_5	3	1	−67%	872	876	0%	213	216	1%
ω_6	5	1	−80%	–	1215	–	–	248	–
ω_7	3	1	−67%	1358	905	−33%	253	216	−15%
ω_8	5	1	−80%	–	1190	–	–	263	–
ω_9	3	1	−67%	656	804	23%	213	208	−2%
ω_{10}	4	1	−75%	1016	932	−8%	291	254	−13%
ω_{11}	3	1	−67%	731	350	−52%	213	97	−54%
ω_{12}	3	1	−67%	785	569	−28%	165	165	0%
ω_{13}	3	1	−67%	1006	1081	7%	212	235	11%
ω_{14}	4	1	−75%	439	922	110%	230	246	7%
ω_{15}	3	1	−67%	1000	1271	27%	224	280	25%
ω_{16}	5	1	−80%	–	1190	–	–	263	–
ω_{17}	3	1	−67%	1068	800	−25%	245	226	−8%
ω_{18}	5	3	−40%	–	231	–	–	145	–
ω_{19}	3	1	−67%	600	975	63%	213	250	17%
ω_{20}	5	3	−40%	–	259	–	–	174	–
ω_{21}	3	1	−67%	1107	1037	−6%	252	213	−15%
ω_{22}	5	1	−80%	–	1151	–	–	235	–
ω_{23}	3	1	−67%	1050	868	−17%	234	210	−10%
ω_{24}	5	1	−80%	–	1190	–	–	263	–
ω_{25}	3	1	−67%	617	503	−18%	157	122	−22%
ω_{26}	3	1	−67%	1101	918	−17%	208	208	0%
ω_{27}	3	1	−67%	927	505	−46%	220	122	−45%
ω_{28}	3	1	−67%	989	773	−22%	212	194	−8%
ω_{29}	3	1	−67%	704	956	36%	213	214	0%
Average:	3.6	1.1	−69%	911	861	−6%	221	210	−5%

delay in the schedule than the minimum cost schedule, and 5% better for the maximum time of delay occurred in a single flight leg. We present the detailed results for these three measures under each disruption scenario in Table 17.

6.4. What if analysis on the number of disrupted aircraft

In order to observe the recovery performances of the minimum cost and the proposed schedules against disruptions caused by the unavailability of multiple aircraft, the number of disrupted aircraft is set to 2 and 45 disruption scenarios are generated in total.

Table 18
Effect of having two disrupted aircraft on the recovery performance.

Disrupted Aircraft	# of Cancelled Flights			Total Time of Delay			Max. Delay in a Flight Leg		
	$\mathcal{P}_1$	$\mathcal{P}_2$	Change	$\mathcal{P}_1$	$\mathcal{P}_2$	Change	$\mathcal{P}_1$	$\mathcal{P}_2$	Change
0, 1	8	2	−75%	1005	2421	141%	213	262	23%
0, 2	8	2	−75%	876	3064	250%	214	262	22%
0, 3	8	2	−75%	824	2657	222%	220	262	19%
0, 4	8	2	−75%	908	2632	190%	202	302	50%
0, 5	8	2	−75%	704	2631	274%	212	302	42%
0, 6	9	2	−78%	600	2795	366%	214	280	31%
0, 7	8	2	−75%	961	2920	204%	213	262	23%
0, 8	10	2	−80%	–	3145	–	–	261	–
0, 9	8	2	−75%	695	2833	308%	213	254	19%
1, 2	6	2	−67%	2018	2992	48%	229	259	13%
1, 3	6	2	−67%	1998	2379	19%	232	259	12%
1, 4	6	2	−67%	1869	2719	45%	229	233	2%
1, 5	6	2	−67%	1869	2360	26%	229	259	13%
1, 6	7	2	−71%	1778	2863	61%	232	369	59%
1, 7	6	2	−67%	2196	2892	32%	242	232	−4%
1, 8	8	2	−75%	1005	2962	195%	213	262	23%
1, 9	6	2	−67%	1988	2514	26%	228	259	14%
2, 3	6	2	−67%	1885	2449	30%	220	257	17%
2, 4	6	2	−67%	1869	2431	30%	213	257	21%
2, 5	6	2	−67%	1860	2431	31%	213	257	21%
2, 6	7	2	−71%	1780	2879	62%	249	261	5%
2, 7	6	2	−67%	2164	2960	37%	258	213	−17%
2, 8	8	2	−75%	990	2988	202%	213	261	23%
2, 9	6	2	−67%	1993	2585	30%	260	257	−1%
3, 4	6	2	−67%	1732	2003	16%	212	220	4%
3, 5	6	2	−67%	1732	2003	16%	212	220	4%
3, 6	7	2	−71%	1643	2407	47%	203	261	29%
3, 7	6	2	−67%	1914	2304	20%	242	220	−9%
3, 8	8	2	−75%	827	2174	163%	220	262	19%
3, 9	6	2	−67%	1840	2178	18%	220	214	−3%
4, 5	6	2	−67%	1613	1950	21%	212	212	0%
4, 6	7	2	−71%	1570	2374	51%	242	261	8%
4, 7	6	2	−67%	1795	2339	30%	242	213	−12%
4, 8	8	2	−75%	707	2163	206%	212	262	24%
4, 9	6	2	−67%	1839	2158	17%	212	215	1%
5, 6	7	2	−71%	1529	2374	55%	256	261	2%
5, 7	6	2	−67%	1795	2339	30%	242	213	−12%
5, 8	8	2	−75%	707	2163	206%	212	262	24%
5, 9	6	2	−67%	1835	2158	18%	212	215	1%
6, 7	7	2	−71%	1698	2728	61%	214	262	22%
6, 8	9	2	−78%	600	2757	360%	214	280	31%
6, 9	7	2	−71%	1709	2401	40%	241	261	8%
7, 8	8	2	−75%	847	2992	253%	214	262	22%
7, 9	6	2	−67%	1914	2441	28%	242	235	−3%
8, 9	8	2	−75%	581	2510	332%	214	261	22%
Average:	7	2	−71%	1461	2543	74%	224	255	13%

In each of these scenarios, 10 flights are disrupted and needed to be recovered. The performances of $\mathcal{P}_1$ and $\mathcal{P}_2$ can be seen in Table 18.

Under each of these scenarios, the number of cancelled flights is significantly lower in $\mathcal{P}_2$ compared to $\mathcal{P}_1$. In addition to that, under the disruption scenario where aircraft 0 and 8 are unavailable, $\mathcal{P}_2$ is able to recover by cancelling only 2 flights while $\mathcal{P}_1$ cancels all of the 10 flights. However, since there is a significant difference between the number of cancelled flights in $\mathcal{P}_1$ and $\mathcal{P}_2$, the corresponding total times of delay in $\mathcal{P}_2$ are significantly higher than $\mathcal{P}_1$. That is why we also look at the maximum time of delay occurred in a flight leg in the schedule as another recovery performance as shown in Table 18. As a result, in the case of two disrupted aircraft, on the average, the proposed schedule $\mathcal{P}_2$ can recover from the disruption with 71% less cancellation than the minimum cost schedule $\mathcal{P}_1$ while the maximum time of delay occurred in a flight leg is increased by only 13% which corresponds to approximately 30 min.

6.5. What if analysis on the aircraft unavailability periods

Until now, we assumed that the aircraft are unavailable for the whole day to generate different disruption scenarios. In order to gain an insight on how the proposed schedules perform against shorter disruptions, we conducted a what if analysis on the aircraft unavailability periods by changing the durations of the aircraft unavailability periods in Table 19. When the aircraft unavailability

Table 19
Description of the aircraft unavailability periods.

Period No.	Time Interval	Duration of Unavailability (hrs)
I	09:00 A.M.–01:00 P.M.	4
II	09:00 A.M.–03:00 P.M.	6
III	09:00 A.M.–05:00 P.M.	8
IV	09:00 A.M.–07:00 P.M.	10
V	09:00 A.M.–09:00 P.M.	12
VI	Whole Day	24

Table 20
Average recovery measures for each unavailability period.

Unavailability Period No.	# of Disrupted Flights		# of Cancelled Flights		Total Time of Delay	
	$\mathcal{P}_1$	$\mathcal{P}_2$	$\mathcal{P}_1$	$\mathcal{P}_2$	$\mathcal{P}_1$	$\mathcal{P}_2$
I	2.6	2.6	0.2	0	761	628
II	3.8	3.6	0.2	0	1100	882
III	4	4	0.3	0	1113	941
IV	4.3	4.2	0.5	0.2	1106	1002
V	4.9	5	2.9	1.4	886	1122
VI	5	5	3.6	1.4	835	1122

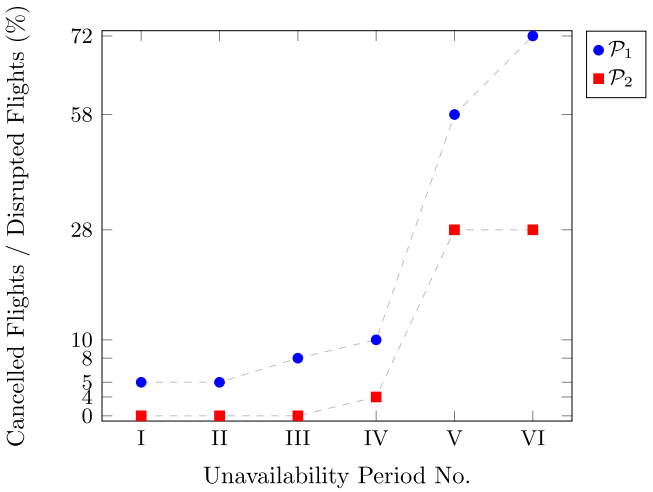

Fig. 5. Effects of aircraft unavailability periods on recovery performance.

period is different than the whole day, the number of disrupted flights in schedules $\mathcal{P}_1$ and $\mathcal{P}_2$ might differ. Therefore, we use the ratio of the number of cancelled flights to the number of disrupted flights as our criterion instead of using only the number of cancelled flights.

In Fig. 5, the effects of the unavailability period on the recovery performances of the 50-flight schedules of $\mathcal{P}_1$ and $\mathcal{P}_2$ are shown. The results are for the average of the 10 disruption scenarios where each of them denotes the unavailability of one aircraft. For the unavailability periods I and II, the minimum cost schedule $\mathcal{P}_1$ cancels 5% of the disrupted flights. However, for the same unavailability periods together with the period III, the proposed schedule $\mathcal{P}_2$ is able to recover all disrupted flights. Similarly, for the remaining unavailability periods, cancellation ratio in $\mathcal{P}_2$ is significantly less than $\mathcal{P}_1$. Moreover, the number of disrupted and cancelled flights as well as the total time of delay can be seen in Table 20 for the average of 10 disruption scenarios for each unavailability period. It is important to note that for shorter unavailability periods, the proposed schedule $\mathcal{P}_2$ could reduce both the number of cancelled flights and total delay simultaneously.

6.6. What if analysis on the airport closures

We first generated disruption scenarios for the 50-flight network where each airport is closed for a certain duration due to an unexpected event. Tables 21–23 report the disruption scenarios that are found to be significant among the airports, namely ORD, DFW and MCI. To observe the recovery performance of the proposed schedules compared to the minimum cost schedules, we evaluate two measures: (1) percentage of the cancelled flights to the disrupted flights and (2) total delay occurred in the schedule after recovery.

Table 21
Airport closure 16:00–17:00.

Time Interval	Airport	Min. Cost Schedule				Proposed Schedule			
		# disrupted flights	# cancelled flights	% cancelled	Total Delay (mins)	# disrupted flights	# cancelled flights	% cancelled	Total Delay (mins)
16:00–17:00	ORD	18	10	56%	78	36	12	33%	117
	DFW	8	4	50%	213	18	0	0%	213
	MCI	4	2	50%	0	4	0	0%	184

Table 22
Airport closure 17:00–20:00.

Time Interval	Airport	Min. Cost Schedule				Proposed Schedule			
		# disrupted flights	# cancelled flights	% cancelled	Total Delay (mins)	# disrupted flights	# cancelled flights	% cancelled	Total Delay (mins)
17:00–20:00	ORD	40	30	75%	108	40	19	48%	166
	DFW	18	9	50%	192	17	0	0%	205
	MCI	4	2	50%	0	4	0	0%	184

Table 23
Airport closure 12:00–18:00.

Time Interval	Airport	Min. Cost Schedule				Proposed Schedule			
		# disrupted flights	# cancelled flights	% cancelled	Total Delay (mins)	# disrupted flights	# cancelled flights	% cancelled	Total Delay (mins)
12:00–18:00	ORD	36	26	72%	118	46	22	48%	114
	DFW	18	9	50%	192	18	0	0%	213
	MCI	4	2	50%	0	4	0	0%	184

In Table 21, the airports are closed for one hour. Even though the duration of the closure is only one hour, number of flights disrupted due to the closure is considerable high in ORD since it is the hub airport. The number of disrupted flights is calculated by counting the number of flights whose assigned flight block time intersects with the closure period. Note that, since the minimum cost and proposed schedules are different from each other in terms of both the routing and the departure and arrival times, the number of disrupted flights varies. That is why the percentage of cancelled flights is used as a performance measure.

In Table 21, half of the disrupted flights are cancelled in the minimum cost schedule when the airports ORD, DFW, and MCI are closed for one hour. However, the proposed schedule cancels 33% of the disrupted flights in ORD and is able to recover all disrupted flights in DFW and MCI. When ORD or MCI is cancelled, we observed a weakly dominating solution for the proposed schedule since the total delay is longer compared to the minimum cost schedule. However, in case of DFW's closure, the proposed schedule performs better or at least the same in terms of both measures.

When the duration of the airport closure is increased, the number of disrupted flights has increased in all three airports, as expected. Tables 22 and 23 show that the proposed schedule is able to recover most of the disrupted flights when ORD, DFW and MCI are closed for longer durations whereas in the minimum cost schedule, over 50% of the flights that are disrupted end up being cancelled. Similarly, we observed longer delays in the proposed schedule as a possible result of the high recovery rates of the disrupted flights. However, we also observed that the proposed schedule yields strongly dominating solution when ORD is closed between 12:00–18:00.

Therefore, it is concluded that the proposed schedules perform better than the minimum cost schedules in terms of the cancellation of the flights and the delay after recovery in case of airport closure as well.

7. Conclusion and future work

We aim to create resilient schedules which are adaptable to uncertain challenges while continuing to stay operational. In addition to the most common goal of the minimization of the operational costs of the airlines, as a significant contribution, we also incorporate the variability into our formulation as a surrogate measure to the resilience. To this end, we formulate the problem as a bi-criteria nonlinear mixed-integer mathematical model with chance constraints. To handle the nonlinearity, we utilize second order cone programming and to handle the chance constraints, we use value-at-risk measure, so that the resulting formulation could be solved by commercial solvers. We also develop a novel math-heuristic algorithm to handle problems with larger flight networks.

As an important contribution, we propose a data-driven methodology to estimate departure and arrival delay probabilities of flights and turnaround times of the aircraft. Through the empirical techniques that we introduce, we are able to capture the trends

in the historical data in our parameter calculations which were previously done in the existing literature in more traditional ways. Moreover, we devise an integrated flight and passenger recovery algorithm to evaluate the performance of our proposed schedules under disruption scenarios in a posterior analysis. Another important contribution is that in case of disruptions caused by the unavailability of the aircraft or airport closures, we provide the decision maker with flexible recovery strategies having different characteristics due to the bi-criteria nature of our recovery performance evaluation.

In our proposed approach, we are not only re-timing the departure times as a result of adjusting the cruise speeds and/or inserting idle times, but also change the flight sequences (that could involve aircraft swapping decisions for different aircraft types) aimed to achieve a balanced distribution of the variability over the aircraft paths in the schedule. Therefore, distributing the variability over the whole schedule increases the resilience of the system to a greater extent than what only idle time insertion can do, since it enlarges the solution space so that different recovery actions could be generated. We observe that the schedules that we propose can recover from the disruptions with less number of flight cancellations compared to the minimum cost schedules. This is another crucial contribution of this study since airlines avoid cancelling flights since the opportunity costs of flight cancellation are high and also the passenger convenience and satisfaction are of great importance to them. We show that by allowing a small deviation from the minimum cost schedule at the schedule generation phase, the potential recovery costs in the future can be reduced significantly. This is a result of the trade-off between the total operational costs and the deviation of the aircraft path variability's which is what initially motivated this study.

In our posterior analysis, we do not consider cancellation and delay in monetary terms, since the results will be quite sensitive to the selected cost parameters. Instead, we focus on the number of flights cancelled and the time of delay occurred (in minutes) as a bi-criteria problem, instead of unifying them into a single criterion in terms of monetary units. For most of the disruption scenarios analyzed in our computational experiments, the schedules that we propose can recover from the disruptions more effectively, and we are able to find strategies which are better in terms of not only one of the performance measures of cancellation or delay but both which is why we introduce the term strongly dominating solutions. As a future research direction, how these measures could be represented in a common unifying function in terms of monetary units for the non-dominated recovery solutions could be investigated. By considering the probability of disruption, additional operational cost, if any, and the estimated costs of flight cancellation and delays, an airline company could assess the benefits of the proposed approach in terms of monetary values for the non-dominated recovery solutions.

The contributions of this study can be extended with several possible future research directions. We assume that the non-cruise time random variables follow Log-Laplace distribution. One possible research idea would be considering other probability distributions which have closed form representations for the random variables. In another possible future study, different data estimation models could be used to estimate the problem parameters. Finally, the performance of our proposed method can also be tested using other recovery algorithms from the literature that captures our bi-criteria formulation with the corresponding operational cost terms that we have used in the proposed mathematical model.

Acknowledgement

The authors thank the editor and two anonymous referees for their constructive comments and suggestions, that significantly improved this paper. This research was partially supported by TUBITAK [Grant 2219].

Appendix A

Integrated Flight and Passenger Recovery Algorithm: To be able to quantify resilience of the schedules and compare the recovery performances of minimum cost schedules and the proposed schedules with each other, a bi-criteria framework is followed. The first performance indicator ξ_1 is the number of cancelled flights after the schedule is recovered from a disruption and the second indicator ξ_2 is the total time of delay occurred after the recovery. Therefore, for a flight schedule $\mathcal{P}$, under the disruption scenario ω which is caused by the availability of an aircraft, we have

$n(\mathcal{P},\omega)$: number of disrupted flights in schedule $\mathcal{P}$ under scenario ω

$\xi_1(\mathcal{P},\omega)$: number of cancelled flights in schedule $\mathcal{P}$ after recovered from disruption ω

$\xi_2(\mathcal{P},\omega)$: total time of delay occurred in schedule $\mathcal{P}$ after recovered from disruption ω.

To generate recovery solutions for flight schedules against disruptions, the Integrated Flight and Passenger Recovery Algorithm is proposed. The main idea of the algorithm is to solve Flight Recovery Model (FRM) first to minimize the number of cancelled flights and then to solve Re-Routing Model (RRM) to route each of the aircraft considering cruise time controllability to minimize the total delay iteratively. In each iteration, eligibility for swapping or accommodating disrupted flights is evaluated to obtain alternative solutions and the algorithm terminates if it cannot find an alternative solution. The pseudo-code can be found in Algorithm 2 in more detail. Sets and parameters that the algorithm utilizes are as follows:

Sets and Parameters:

E_D : set of disrupted flight blocks

E_N : set of existing, i.e., non-disrupted flight blocks

E : set of flight blocks, i.e., $E_D \cup E_N$

F_i : set of flights in flight block $i \in E$

t^i : aircraft operating the flight block $i \in E$

c^i : number of flights in the flight block $i \in E$

a_i^t : 1 if flight block $i \in E_D$ can be accommodated in the path of aircraft $t \in T \backslash t^i$, and 0 o.w.

b_{ij} : 1 if flight blocks $i \in E_D$ and $j \in E_N$ can be swapped, and 0 o.w.

$c_i^{t^i}$: 1 if flight block $i \in E_D$ can be recovered with delay in the path of aircraft t^i, and 0 o.w.

Algorithm 2 Integrated Flight and Passenger Recovery Algorithm (IAPRA)

INITIALIZATION:
Define the set of problems as $\mathcal{P} := \emptyset$ and the set of solutions as $\mathcal{S} := \emptyset$.
Take E_D, E_N and F_i as input. Calculate the matrices $[a]_i^t$ and $[b]_{ij}$.
Denote the problem with these matrices as P_0 and let the problem set $\mathcal{P} \leftarrow \{P_0\}$.
STEP 1: Solve (FRM) for problem $P_k \in \mathcal{P}$. Update $\mathcal{P} \leftarrow \mathcal{P} \backslash P_k$.
Let S represent the solution. Update $\mathcal{S} \leftarrow \mathcal{S} \cup S$.
In the solution S:
for each $i \in E_D$ **do**
  for each $t \in T$ **do**
    if $accom_i^t = 1$ **then**
      Create problem P by updating $a_i^t \leftarrow 0$ and let $\mathcal{P} \leftarrow \mathcal{P} \cup \{P\}$.
    else if $swap_{ij} = 1$ **then**
      Create problem P by updating $b_{ij} \leftarrow 0$ and let $\mathcal{P} \leftarrow \mathcal{P} \cup \{P\}$.
    end if
  end for
end for
Go to Step 2.
STEP 2: Solve (RRM) for solution S. Report the solution.
if $\mathcal{S} \neq \emptyset$ **then**
  Go to Step 1.
else
  Stop. Report $\mathcal{S}$ as the set of recovery solutions.
end if

A.1. Flight recovery model

The parameters a_i^t and b_{ij}, which denote the eligibility for accommodating and swapping a flight block, are calculated by simply checking if the disrupted flight block can be compressed by speeding up the assigned aircraft if necessary and accommodated into the existing schedule by utilizing the idle times and by compressing the other existing flights. The detailed explanations can be found in Algorithms 3 and 4. We introduce the following new decision variables:

$cancel_i$: 1 if flight block i is cancelled, $i \in E_D$, and 0 o.w.

$swap_{ij}$: 1 if flight blocks $i \in E_D$ and $j \in E_N$ are swapped, and 0 o.w.

$accom_i^t$: 1 if flight block $i \in E_D$ is accommodated in the path of aircraft $t \in T \backslash t^i$, and 0 o.w.

$delay_i^{t^i}$: 1 if flight block $i \in E_D$ is recovered with delay in the path of aircraft t^i, and 0 o.w.

Flight Recovery Model (FRM):

$$\xi_1 = \min \sum_{i \in E_D} c^i \times cancel_i + \sum_{i \in E_D} \sum_{j \in E_N} c^j \times swap_{ij} \tag{40}$$

$$\text{s.t.} \quad cancel_i + \sum_{j \in E_N} swap_{ij} + \sum_{t \in T \backslash t^i} accom_i^t + delay_i^{t^i} = 1 \quad \forall i \in E_D \tag{41}$$

$$\sum_{i \in E_D} swap_{ij} \leq 1 \quad \forall j \in E_N \tag{42}$$

$$\sum_{i \in E_D} accom_i^t \leq 1 \quad \forall t \in T \backslash t^i \tag{43}$$

$$accom_i^t \leq a_i^t \quad \forall i \in E_D,\ t \in T \backslash t^i \tag{44}$$

$$swap_{ij} \leq b_{ij} \quad \forall i \in E_D,\ j \in E_N \tag{45}$$

$$delay_i^{t^i} \leq c_i^{t^i} \quad \forall i \in E_D \tag{46}$$

$$swap_{ij} \in \{0, 1\} \quad \forall i \in E_D,\ j \in E_N \tag{47}$$

$$accom_i^t \in \{0,1\} \qquad \forall i \in E_D,\ t \in T \backslash t^i \tag{48}$$

$$delay_i^{t^i} \in \{0,1\} \qquad \forall i \in E_D \tag{49}$$

The objective function (40) minimizes the number of cancelled flights. Constraints (41) ensure that a disrupted flight block can either be cancelled, swapped with a non-disrupted flight block, recovered in the path of its originally assigned aircraft with a delayed departure or accommodated into the existing path of another aircraft. Constraints (42) ensure that a non-disrupted flight block can be swapped with at most one disrupted flight block. Constraints (43) ensure that the existing path of an aircraft can accommodate at most one disrupted flight block. Constraints (44)–(46) make sure that accommodating and swapping a disrupted flight block are possible if the corresponding parameters are equal to one. Constraints (47)–(49) are binary constraints. Note that it is not necessary to have binary constraints for variable $cancel_i$ due to the constraints (41) and (47)–(49).

A.2. Re-routing model

After (FRM) is solved to obtain the minimum number of flight cancellations and the corresponding recovery decisions, for each aircraft $t \in T$ with changed flight block assignments, we define the following updated notation associated with the re-routing model:

Sets and Parameters:

F^t : set of flights assigned to aircraft t

A^t : set of all possible flight pairs assigned to aircraft t

$US^i,\ DS^i$: upstream and downstream flights of flight $i \in F^t$

TA_{ij} : turnaround time needed to prepare aircraft between $(i,j) \in A^t$

d_i^{min} : departure time of flight i obtained in ε-CM, $i \in F^t$

d_i^{max} : upper bound for departure time of flight $i \in F^t$

$f_i^l,\ f_i^u$: lower and upper bounds for cruise time of flight $i \in F^t$

Decision Variables:

d_i : departure time of flight $i \in F^t$

s_i : idle time of aircraft after flight $i \in F^t$

f_i : cruise time of flight $i \in F^t$

x_{ij} : 1 if flight i is followed by flight j, $(i,j) \in A^t$, and 0 o.w.

y_i : 1 if flight i is the first flight performed by aircraft t, $i \in F^t$, and 0 o.w.

z_i : 1 if flight i is the last flight performed by aircraft t, $i \in F^t$, and 0 o.w.

Algorithm 3 Algorithm to Check Eligibility for Swapping Disrupted and Existing Flight Blocks.

for each $i \in E$ **do**
  Let $block^i := \sum_{k \in F_i} f_k^l$ denote the block time of flight block i.
  Let $cruise^i := \sum_{k \in F_i} f_k$ denote the total cruise time of flight block i.
  Let $idle^i := \sum_{k \in F_i} s_k$ denote the total idle time in flight block i.
  if $c^i = 1$ **then**
    Let $slack^i$ denote the time until midnight after flight block i.
  end if
end for
for each $i \in E$ **do**
  for each $i \in E$ **do**
    if $t^i = t^j$ **then**
      $b_{ij} \leftarrow 0$
    else if $c^j = 2$ **and** $block^i \le cruise^j + idle^j$ **then**
      $b_{ij} \leftarrow 1$
    else if $c^j = 1$ **and** $block^i \le cruise^j + idle^j + slack^j$ **then**
      $b_{ij} \leftarrow 1$
    else
      $b_{ij} \leftarrow 0$
    end if
  end for
end for

Algorithm 4 Algorithm to Check Eligibility for Accommodating a Disrupted Flight Block into an Existing Path.

for each $i \in E$ **do**
  Let $block^i := \sum_{k \in F_i} f_k^l$ denote the block time of flight block i.
  Let $cruise^i := \sum_{k \in F_i} f_k$ denote the total cruise time of flight block i.
  Let $idle^i := \sum_{k \in F_i} s_k$ denote the total idle time in flight block i.
  if $c^i = 1$ **then**
    Let $slack^i$ denote the time until midnight after flight block i.
  end if
end for
for each $t \in T$ **do**
  Let $slackInPath^t$ denote the slack time that can be created in the path of aircraft t.
  $slackInPath^t \leftarrow 0$
  for each $i \in E$ **do**
    if $t^i = t$ **then**
      if $c^i = 2$ **then**
        $slackInPath^t \leftarrow slackInPath^t + idle^i + cruise^i - block^i$
      else if $c^i = 1$ **then**
        $slackInPath^t \leftarrow slackInPath^t + idle^i + slack^i + cruise^i - block^i$
      end if
    end if
  end for
end for
for each $i \in E$ **do**
  for each $t \in T$ **do**
    if $t^i = t$ **then**
      $a_i^t \leftarrow 0$
    else if $c^j = 2$ **and** $block^i + turnTime \le slackInPath^t$ **then**
      $a_i^t \leftarrow 1$
    else
      $a_i^t \leftarrow 0$
    end if
  end for
end for

Re-Routing Model:

$$\xi_2 = \min \sum_{i \in F^t} \left(d_i - d_i^{min}\right) \tag{50}$$

$$\text{s.t.} \sum_{j \in US^i} x_{ji} + y_i - \sum_{j \in DS^i} x_{ij} - z_i = 0 \qquad \forall i \in F^t \tag{51}$$

$$\sum_{j \in US^i} x_{ji} + y_i = 1 \qquad \forall i \in F^t \tag{52}$$

$$\sum_{i \in F^t} y_i \le 1 \tag{53}$$

$$f_i^l \le f_i \le f_i^u \qquad \forall i \in F^t \tag{54}$$

$$d_i^{min} \le d_i \le d_i^{max} \qquad \forall i \in F^t \tag{55}$$

$$\text{IF } x_{ij} = 1 \text{ THEN}$$

$$d_j - d_i - TA_{ij} - f_i - \text{VaR}_{1-\gamma_i}(NC_i) - s_i = 0 \qquad \forall (i,j) \in A^t \tag{56}$$

$$\sum_{i \in F^t} f_i \le \lambda_t \tag{57}$$

$$s_i \ge 0 \qquad \forall i \in F^t \tag{58}$$

$$x_{ij} \in \{0,1\} \qquad \forall (i,j) \in A^t \tag{59}$$

$$y_i \in \{0,1\} \qquad \forall i \in F^t \tag{60}$$

The objective function (50) minimizes the total delay occurred in the schedule by summing the differences between the departure times of the flights and the published departure times over all flights. Constraints (51) are the network balance constraints and together with the constraints (52), they determine the aircraft routes and assign individual aircraft to those routes. Constraint (53) ensures that there is at most one aircraft route is assigned to an aircraft. Constraint sets (54) and (55) limit the cruise time controllability and the departure times for each flight, respectively. Constraints (56) are the chance constraints which are the same as in ε-model. Constraint (57) is the maintenance feasibility constraint. Constraints (58)–(60) are domain constraints for the idle time variables and binary variables.

Table 24
Schedules for 150 flight network.

Tail No.	Aircraft No.	Minimum Cost Schedule $\mathcal{P}_1$					Proposed Schedule $\mathcal{P}_2$				
		Flight No.	Origin	Dest.	Departure Time	Arrival Time	Flight No.	Origin	Dest.	Departure Time	Arrival Time
N678UA	0	100	ORD	BOS	07:38	09:22	Same				
		101	BOS	ORD	10:15	12:18					
		27	ORD	LGA	13:24	15:06					
		58	LGA	ORD	17:16	19:13					
		114	ORD	EWR	20:20	22:49					
N802WA	1	125	ORD	DFW	09:45	11:15	87	ORD	DFW	09:45	11:15
		71	DFW	ORD	12:34	13:58	143	DFW	ORD	12:34	13:58
		127	ORD	STL	15:17	16:50	127	ORD	STL	17:22	18:55
		23	STL	ORD	17:42	19:08	23	STL	ORD	19:47	21:13
		84	ORD	LGA	20:40	22:22	84	ORD	LGA	22:46	00:28
N805WA	2	65	ORD	MSP	07:15	08:19	65	ORD	MSP	07:15	08:20
		66	MSP	ORD	09:15	10:16	66	MSP	ORD	09:16	10:17
		47	ORD	DFW	11:23	12:53	47	ORD	DFW	11:23	12:53
		98	DFW	ORD	14:35	15:59	98	DFW	ORD	14:34	15:58
		49	ORD	DEN	17:30	19:20	109	ORD	LGA	17:29	19:11
N309US	3	15	ORD	MSP	07:15	08:19	15	ORD	MSP	07:15	08:20
		16	MSP	ORD	09:15	10:16	16	MSP	ORD	09:16	10:17
		12	ORD	DFW	11:23	12:53	12	ORD	DFW	11:23	12:53
		63	DFW	ORD	14:35	15:59	63	DFW	ORD	14:34	15:58
		99	ORD	DEN	17:30	19:20	104	ORD	DFW	17:29	18:59
N334NW	4	45	ORD	MCI	07:15	08:15	45	ORD	MCI	07:15	08:16
		46	MCI	ORD	09:12	10:12	46	MCI	ORD	09:12	10:11
		97	ORD	DFW	11:22	12:52	97	ORD	DFW	11:21	12:51
		48	DFW	ORD	14:35	15:59	48	DFW	ORD	14:34	15:58
		14	ORD	DEN	17:30	19:20	4	ORD	LGA	17:29	19:11
N312US	5	80	ORD	DFW	07:29	08:59	Same				
		136	DFW	ORD	10:29	11:53					
		2	ORD	DFW	13:34	15:04					
		88	DFW	ORD	17:00	18:24					
		74	ORD	SAN	19:15	20:54					
N681UA	6	50	ORD	LGA	07:48	09:30	50	ORD	LGA	07:47	09:29
		1	LGA	ORD	10:23	12:20	1	LGA	ORD	10:22	12:20
		102	ORD	LGA	13:15	14:57	115	ORD	LAX	13:14	15:14
		133	LGA	ORD	15:56	17:53	116	LAX	ORD	16:14	17:56
		29	ORD	BOS	19:00	20:44	29	ORD	BOS	20:44	22:28
N807TR	7	135	ORD	DFW	07:29	08:59	Same				
		91	DFW	ORD	10:18	11:43					
		32	ORD	AUS	13:49	15:31					
		83	AUS	ORD	17:21	18:58					
		144	ORD	LGA	20:20	22:02					
N695UA	8	85	ORD	LGA	08:10	09:52	Same				
		36	LGA	ORD	10:45	12:42					
		77	ORD	LGA	13:37	15:19					
		78	LGA	ORD	16:13	18:10					
		19	ORD	BOS	21:30	23:14					
N422BN	9	20	ORD	DFW	09:45	11:15	Same				
		126	DFW	ORD	12:20	13:44					
		147	ORD	ATL	14:36	15:56					
		148	ATL	ORD	16:58	18:27					
		94	ORD	SAN	20:00	21:39					
N966UA	10	120	ORD	MIA	08:45	10:22	120	ORD	MIA	08:45	10:22
		121	MIA	ORD	11:52	13:36	121	MIA	ORD	11:53	13:37
		7	ORD	LGA	14:32	16:14	7	ORD	LGA	14:32	16:14
		93	LGA	ORD	17:25	19:22	93	LGA	ORD	17:25	19:23
		109	ORD	LGA	21:00	22:42	49	ORD	DEN	21:01	22:51

(*continued on next page*)

Appendix B

See Tables 24 and 25.

Table 24 (*continued*).

Tail No.	Aircraft No.	Minimum Cost Schedule $\mathcal{P}_1$					Proposed Schedule $\mathcal{P}_2$				
		Flight No.	Origin	Dest.	Departure Time	Arrival Time	Flight No.	Origin	Dest.	Departure Time	Arrival Time
N305FA	11	105	ORD	MCI	06:45	07:45	Same				
		61	MCI	ORD	09:01	10:01					
		62	ORD	DFW	11:21	12:51					
		13	DFW	ORD	14:35	15:59					
		64	ORD	DEN	17:30	19:20					
N573UA	12	95	ORD	MCI	07:15	08:15	95	ORD	MCI	07:15	08:16
		11	MCI	ORD	09:13	10:13	11	MCI	ORD	09:13	10:13
		107	ORD	MSP	12:19	13:24	107	ORD	MSP	12:19	13:24
		108	MSP	ORD	17:06	18:07	108	MSP	ORD	17:06	18:07
		104	ORD	DFW	19:00	20:30	99	ORD	DEN	19:01	20:51
N438BN	13	25	ORD	DFW	08:06	09:36	Same				
		81	DFW	ORD	10:30	11:54					
		117	ORD	SAN	12:45	14:23					
		68	SAN	ORD	17:06	18:29					
		89	ORD	LGA	20:20	22:02					
N335NW	14	115	ORD	LAX	06:46	08:46	102	ORD	LGA	06:46	08:28
		116	LAX	ORD	09:40	11:22	133	LGA	ORD	09:21	11:19
		67	ORD	SAN	12:15	13:53	67	ORD	SAN	12:28	14:07
		118	SAN	ORD	16:51	18:14	118	SAN	ORD	17:05	18:28
		119	ORD	MIA	20:20	21:57	119	ORD	MIA	20:34	22:11

Table 25
Cont.'d from Table 24.

Tail No.	Aircraft No.	Minimum Cost Schedule $\mathcal{P}_1$					Proposed Schedule $\mathcal{P}_2$				
		Flight No.	Origin	Dest.	Departure Time	Arrival Time	Flight No.	Origin	Dest.	Departure Time	Arrival Time
N317US	15	40	ORD	DFW	07:45	09:15	132	ORD	LGA	07:45	09:27
		56	DFW	ORD	10:23	11:47	28	LGA	ORD	10:35	12:32
		37	ORD	DFW	13:34	15:04	37	ORD	DFW	16:48	18:18
		53	DFW	ORD	17:21	18:45	53	DFW	ORD	20:35	21:59
		44	ORD	SAN	20:00	21:39	44	ORD	SAN	23:14	00:53
N967UA	16	140	ORD	LGA	08:10	09:52	140	ORD	LGA	08:10	09:52
		51	LGA	ORD	10:45	12:42	51	LGA	ORD	10:44	12:42
		92	ORD	LGA	14:17	15:59	92	ORD	LGA	14:17	15:59
		43	LGA	ORD	17:17	19:15	43	LGA	ORD	17:17	19:15
		4	ORD	LGA	20:20	22:02	14	ORD	DEN	20:20	22:10
N801WA	17	5	ORD	DFW	07:45	09:15	142	ORD	DFW	07:45	09:15
		76	DFW	ORD	10:49	12:13	38	DFW	ORD	10:49	12:13
		137	ORD	AUS	13:49	15:31	137	ORD	AUS	17:38	19:20
		138	AUS	ORD	17:21	18:58	138	AUS	ORD	21:10	22:47
		34	ORD	LGA	20:40	22:22	34	ORD	LGA	00:29	02:11
N969UA	18	145	ORD	EWR	07:24	09:53	145	ORD	EWR	07:24	09:53
		146	EWR	ORD	10:45	13:25	146	EWR	ORD	10:45	13:25
		122	ORD	FLL	15:45	17:28	82	ORD	AUS	15:45	17:27
		123	FLL	ORD	18:20	20:12	33	AUS	ORD	18:19	19:56
		149	ORD	EWR	21:03	23:32	149	ORD	EWR	21:40	00:09
N727YK	19	75	ORD	DFW	08:32	10:02	Same				
		31	DFW	ORD	10:55	12:19					
		22	ORD	STL	15:17	16:50					
		128	STL	ORD	17:42	19:08					
		54	ORD	LGA	20:20	22:02					
N821AU	20	110	ORD	EWR	07:24	09:53	Same				
		111	EWR	ORD	10:45	13:25					
		57	ORD	LGA	14:26	16:08					
		8	LGA	ORD	17:24	19:22					
		69	ORD	BOS	21:30	23:14					

(*continued on next page*)

Table 25 (*continued*).

Tail No.	Aircraft No.	Minimum Cost Schedule $\mathcal{P}_1$					Proposed Schedule $\mathcal{P}_2$				
		Flight No.	Origin	Dest.	Departure Time	Arrival Time	Flight No.	Origin	Dest.	Departure Time	Arrival Time
N319US	21	55	ORD	DFW	07:45	09:15	55	ORD	DFW	07:45	09:15
		41	DFW	ORD	10:23	11:47	41	DFW	ORD	10:23	11:47
		82	ORD	AUS	13:49	15:31	122	ORD	FLL	13:50	15:32
		33	AUS	ORD	17:18	18:55	123	FLL	ORD	17:20	19:12
		59	ORD	SAN	20:00	21:39	59	ORD	SAN	22:20	23:58
N240AT	22	35	ORD	LGA	08:07	09:49	35	ORD	LGA	08:07	09:49
		141	LGA	ORD	10:41	12:39	141	LGA	ORD	10:41	12:39
		132	ORD	LGA	13:34	15:16	40	ORD	DFW	13:34	15:04
		28	LGA	ORD	16:09	18:06	56	DFW	ORD	15:57	17:21
		79	ORD	BOS	19:01	20:44	79	ORD	BOS	18:38	20:22
N164TS	23	90	ORD	DFW	07:45	09:15	90	ORD	DFW	07:45	09:15
		131	DFW	ORD	10:47	12:11	131	DFW	ORD	10:47	12:11
		87	ORD	DFW	13:36	15:06	125	ORD	DFW	13:37	15:07
		143	DFW	ORD	17:21	18:45	71	DFW	ORD	17:22	18:46
		39	ORD	LGA	20:20	22:02	39	ORD	LGA	21:14	22:56
N656CS	24	0	ORD	LGA	08:10	09:52					
		86	LGA	ORD	10:45	12:42					
		42	ORD	LGA	14:00	15:42	Same				
		103	LGA	ORD	16:35	18:32					
		134	ORD	BOS	19:27	21:11					
N784CK	25	10	ORD	MCI	07:15	08:15	10	ORD	MCI	07:15	08:16
		106	MCI	ORD	09:08	10:08	106	MCI	ORD	09:09	10:08
		142	ORD	DFW	13:34	15:04	5	ORD	DFW	13:35	15:05
		38	DFW	ORD	17:21	18:45	76	DFW	ORD	17:23	18:47
		124	ORD	ATL	22:00	23:20	124	ORD	ATL	23:29	00:49
N320US	26	130	ORD	DFW	08:45	10:15	52	ORD	DFW	08:45	10:15
		26	DFW	ORD	11:09	12:33	3	DFW	ORD	11:09	12:33
		112	ORD	ATL	13:30	14:50	112	ORD	ATL	14:33	15:53
		113	ATL	ORD	16:51	18:20	113	ATL	ORD	17:54	19:23
		9	ORD	SAN	20:00	21:39	9	ORD	SAN	21:03	22:41
N336NW	27	60	ORD	MCI	07:15	08:15					
		96	MCI	ORD	09:13	10:13					
		17	ORD	SAN	11:49	13:27	Same				
		18	SAN	ORD	16:46	18:10					
		24	ORD	SAN	19:00	20:39					
N353PA	28	30	ORD	DFW	07:29	08:59	30	ORD	DFW	07:29	08:59
		6	DFW	ORD	10:18	11:43	6	DFW	ORD	10:19	11:43
		52	ORD	DFW	13:34	15:04	130	ORD	DFW	13:35	15:05
		3	DFW	ORD	17:00	18:24	26	DFW	ORD	17:08	18:32
		129	ORD	SAN	19:15	20:54	129	ORD	SAN	19:30	21:08
N355PA	29	70	ORD	DFW	09:45	11:15					
		21	DFW	ORD	12:34	13:58					
		72	ORD	STL	15:17	16:50	Same				
		73	STL	ORD	17:42	19:08					
		139	ORD	LGA	20:40	22:22					

Appendix C. Posteriori analysis on non-cruise time parameters

C.1. What if analysis on β

Increasing the value of β significantly increases the variance values of our Log-Laplace random variables and the deviation of the path variabilities. To observe whether the recovery performance of the schedules is affected by the value of β, a posterior analysis is conducted as summarized in Table 26. In each of the scenarios and levels for β, the proposed schedule $\mathcal{P}_2$ yields either strongly-dominating or non-dominated recovery solutions. In summary, $\mathcal{P}_2$ is "better" by 61% and 69% in terms of the number of cancelled flights for $\beta = 0.01$ and $\beta = 0.05$, respectively. However, it faces 34% and 36% more time of delay compared to $\mathcal{P}_1$ in each setting.

Table 26
Effect of β on the recovery performance.

Disruption Scenario	$\beta = 0.01$				$\beta = 0.05$			
	$\mathcal{P}_1$		$\mathcal{P}_2$		$\mathcal{P}_1$		$\mathcal{P}_2$	
	ξ_1	ξ_2	ξ_1	ξ_2	ξ_1	ξ_2	ξ_1	ξ_2
ω_0	5	–	1	1416	5	–	2	1618
ω_1	3	891	1	1166	3	1121	1	1442
ω_2	3	990	1	1414	3	1003	1	1414
ω_3	3	905	1	925	3	1008	1	925
ω_4	3	791	1	892	3	879	1	1188
ω_5	3	841	1	898	3	961	1	892
ω_6	5	–	3	1012	4	600	1	1221
ω_7	3	847	1	1437	3	847	1	1470
ω_8	5	–	3	1125	5	–	1	1192
ω_9	3	581	1	937	3	959	1	1136
Average:	3.6	835	1.4	1122	3.5	922	1.1	1250

Table 27
Effect of α on the schedule generation.

α	Min. Cost Schedule $\mathcal{P}_1$		Proposed Schedule $\mathcal{P}_2$			Imp. in F_2
	F_1 ($)	F_2	F_1 ($)	F_2	Inserted Idle Time (mins)	
ln(20)	796294	5.32	874284	3.24	555	39%
ln(25)	796270	6.75	861300	4.25	459	37%

Table 28
Effect of α on the recovery performance.

Disruption Scenario	$\alpha = \ln(20)$				$\alpha = \ln(25)$			
	$\mathcal{P}_1$		$\mathcal{P}_2$		$\mathcal{P}_1$		$\mathcal{P}_2$	
	ξ_1	ξ_2	ξ_1	ξ_2	ξ_1	ξ_2	ξ_1	ξ_2
ω_0	5	–	1	1416	5	–	1	1266
ω_1	3	891	1	1166	3	1163	1	785
ω_2	3	990	1	1414	3	903	1	1127
ω_3	3	905	1	925	3	702	1	739
ω_4	3	791	1	892	3	702	1	739
ω_5	3	841	1	898	3	739	1	791
ω_6	5	–	3	1012	3	905	1	867
ω_7	3	847	1	1437	4	560	1	740
ω_8	5	–	3	1125	5	–	1	1342
ω_9	3	581	1	937	3	838	1	917
Average:	3.6	835	1.4	1122	3.5	814	1	913

C.2. What if analysis on α

Increasing the value of α increases the average duration of the non-cruise times, and results in less idle time insertion possibility due to the limited time of the aircraft on a day as shown in Table 27. When $\alpha = \ln(20)$, the algorithm is able to insert a total of 555 min idle time to the minimum cost schedule to obtain $\mathcal{P}_2$, whereas when $\alpha = \ln(25)$, the inserted idle time drops to 459 min.

In order to find out whether increasing α increases the recovery performance or not, we conducted a posterior analysis and the results against each disruption scenario can be found in Table 28. Although the recovery performance of the schedules is expected to be improved as the idle time insertion increases, the results show that when $\alpha = \ln(25)$, the difference between the recovery performances of the proposed schedule and the minimum cost schedule is higher. On the average, when $\alpha = \ln(25)$, $\mathcal{P}_2$ is able to recover from the schedules by cancelling 2.5 less flights than $\mathcal{P}1$, whereas this value is 2.2 if we have $\alpha = \ln(20)$. Similarly, total time of delay in $\mathcal{P}_2$ is significantly lower if $\alpha = \ln(25)$. The reason for the schedules with high setting for α performing better against disruptions is due to the better placement of idle times into the flight schedule by considering the variability of each flight leg.

References

AhmadBeygi, S., Cohn, A., Lapp, M., 2010. Decreasing airline delay propagation by reallocating scheduled slack. IEEE Trans. 42, 478–489. http://dx.doi.org/10.1080/07408170903468605.

Aktürk, M.S., Atamtürk, A., Gürel, S., 2014. Aircraft rescheduling with cruise speed control. Oper. Res. 62, 829–845. http://dx.doi.org/10.1287/opre.2014.1279.

Arıkan, U., Gürel, S., Aktürk, M.S., 2017. Flight network-based approach for integrated airline recovery with cruise speed control. Transp. Sci. 51, 1259–1287. http://dx.doi.org/10.1287/trsc.2016.0716.

Arora, S.D., Mathur, S., 2020. Effect of airline choice and temporality on flight delays. J. Air Transp. Manag. 86, 101813. http://dx.doi.org/10.1016/j.jairtraman.2020.101813.

Ben Ahmed, M., Ghroubi, W., Haouari, M., Sherali, H.D., 2017. A hybrid optimization-simulation approach for robust weekly aircraft routing and retiming. Transp. Res. C Emerg. Technol. 84, 1–20. http://dx.doi.org/10.1016/j.trc.2017.07.010.

Bureau of Transportation Statistics, 2020. T-100 domestic market data. Available at: https://www.bts.gov/browse-statistical-products-and-data/bts-publications/. (Accessed August 2021).

Bureau of Transportation Statistics, 2021. Airline on-time performance data. Available at: https://www.transtats.bts.gov/Fields.asp?gnoyr_VQ=FGJ. (Accessed August 2021).

Cadarso, L., De Celis, R., 2017. Integrated airline planning: Robust update of scheduling and fleet balancing under demand uncertainty. Transp. Res. C Emerg. Technol. 81, 227–245. http://dx.doi.org/10.1016/j.trc.2017.06.003.

Clark, K.L., Bhatia, U., Kodra, E.A., Ganguly, A.R., 2018. Resilience of the U.S. national airspace system airport network. IEEE Trans. Intell. Transp. Syst. 19, 3785–3794. http://dx.doi.org/10.1109/tits.2017.2784391.

Cook, A., Delgado, L., Tanner, G., Cristobal, S., 2016. Measuring the cost of resilience. J. Air Transp. Manag. 56, 38–47. http://dx.doi.org/10.1016/j.jairtraman.2016.02.007.

Deshpande, V., Arıkan, M., 2012. The impact of airline flight schedules on flight delays. Manuf. Serv. Oper. Manag. 14, 423–440. http://dx.doi.org/10.1287/msom.1120.0379.

Duran, A.S., Gürel, S., Aktürk, M.S., 2015. Robust airline scheduling with controllable cruise times and chance constraints. IIE Trans. 47, 64–83. http://dx.doi.org/10.1080/0740817X.2014.916457.

EUROCONTROL, 2012. User Manual for the Base of Aircraft Data (Bada) Revision 3.10. Tech. Rep. 12/04/10-45, EEC Technical/Scientific, Eurocontrol, Eurocontrol Experimental Centre, B.P., Bretigny-sur-Orge, France, 15, F-91222.

Evler, J., Asadi, E., Preis, H., Fricke, H., 2021. Airline ground operations: Schedule recovery optimization approach with constrained resources. Transp. Res. C Emerg. Technol. 128 (10129), http://dx.doi.org/10.1016/j.trc.2021.103129.

Faraway, J.J., 2016. Extending the Linear Model with R: Generalized Linear, Mixed Effects and Nonparametric Regression Models, second ed. CRC Press Taylor & Francis Group.

Gürkan, H., Gürel, S., Aktürk, M.S., 2016. An integrated approach for airline scheduling, aircraft fleeting and routing with cruise speed control. Transp. Res. C Emerg. Technol. 68, 38–57. http://dx.doi.org/10.1016/j.trc.2016.03.002.

Hassan, L.K., Santos, B.F., Vink, J., 2020. Airline distruption management: A literature review and practical challenges. Comput. Oper. Res. 127, 105137. http://dx.doi.org/10.1016/j.cor.2020.105137.

Janić, M., 2015. Modelling the resilience, friability and costs of an air transport network affected by a large-scale disruptive event. Transp. Res. A. 71, 1–16. http://dx.doi.org/10.1016/j.trd.2019.02.011.

Lambelho, M., Mitici, M., Pickup, S., Marsden, A., 2020. Assessing strategic flight schedules at an airport using maching learning-based flight delay and cancellation predictions. J. Air Transp. Manag. 82, 101737. http://dx.doi.org/10.1016/j.jairtraman.2019.101737.

Lufthansa, 2018. From robust scheduling to resilient scheduling and operations - optimize on-time performance based on delay risk prediction. Available at: https://www.lhsystems.com/blog-entry/robust-scheduling-resilient-scheduling-and-operations-optimize-time-performance-based. (Accessed August 2021).

Petersen, J.D., Sölveling, G., Clarke, J.-P., Johnson, E.L., Shebaloc, S., 2021. An optimization approach to airline integrated recovery. Transp. Sci. 46, 482–500.

Prakash, A.A., 2020. Algorithms for most reliable routes on stochastic and time-dependent networks. Transp. Res. B Methodol. 138, 202–220.

Şafak, Ö., Çavuş, Ö., Aktürk, M.S., 2018. Multi-stage airline scheduling problem with stochastic passenger demand and non-cruise times. Transp. Res. B Methodol. 114, 39–67. http://dx.doi.org/10.1016/j.trb.2018.05.012.

Sohoni, M., Lee, Y.-C., Klabjan, D., 2011. Robust airline scheduling under block-time uncertainty. Transp. Sci. 45, 451–464. http://dx.doi.org/10.1287/trsc.1100.0361.

T'kindt, V., Billaut, J.-C., 2006. Multicriteria Scheduling: Theory, Models and Algorithms. Springer.

U.S. Department of Transportation, 2021. Federal aviation administration. Aircraft Registry Database. Available at: https://registry.faa.gov/aircraftinquiry/. (Accessed August 2021).

Wang, X., Brownlee, A.E.I., Woodward, J.R., Weiszer, M., Mahfouf, M., Chen, J., 2021. Aircraft taxi time prediction: Feature importance and their implications. Transp. Res. C Emerg. Technol. 124, 102892. http://dx.doi.org/10.1016/j.trc.2020.102892.

Wang, Y., Zhan, J., Xu, X., Li, L., Chen, P., Hansen, M., 2019. Measuring the resilience of an airport network. Chinese J. Aeronaut. 32, 2694–2705. http://dx.doi.org/10.1016/j.cja.2019.08.023.

Wong, A., Tan, S., Chandramouleeswaran, K.R., Tran, H.T., 2020. Data-driven analysis of resilience in airline networks. Transp. Res. E Logist. Transp. Rev. 143, 102068. http://dx.doi.org/10.1016/j.tre.2020.102068.

Xu, Y., Wandelt, S., Sun, X., 2021. Airline integrated robust scheduling with a variable neighborhood search based heuristic. Transp. Res. B Methodol. 149, 181–203. http://dx.doi.org/10.1016/j.trb.2021.05.005.